Structural and Magnetic Properties of Dicopper(II) Complexes of Polydentate Diazine Ligands

Laurence K. Thompson,*,† Zhiqiang Xu,† Andrés E. Goeta,‡ Judith A. K. Howard,‡ Howard J. Clase,† and David O. Miller†

Departments of Chemistry, Memorial University of Newfoundland, St. John's, Newfoundland A1B 3X7, Canada, and University of Durham, Durham DH1 3LE, U.K.

Received December 3, 1997

A series of dinuclear copper(II) complexes of three polydentate diazine ligands (PAHAP, PHMAP, and PAHOX) is reported. The PAHAP and PHMAP complexes involve tetradentate ligand coordination with an N−N bridge between the metal centers. For PAHOX, one case involves oxime (N−O) bridges, while, in another, μ_2-SO_4 bridges are present. Free rotation of the copper magnetic planes around the N−N bond occurs for the PAHAP complexes and is influenced by secondary ligand steric effects (cis), but, for PHMAP, additional coordination fixes the complex in a trans configuration. Preliminary structures are reported for $[Cu_2(PAHAP)(NCS)_4(DMF)_2]\cdot 2DMF$ (**1**) and $[Cu_2(PAHAP)(bipy)_2(NO_3)_2](NO_3)_2\cdot 4H_2O$ (**2**), and full structures are reported for $[Cu_2(PAHAP)(aln)_2(H_2O)_2](NO_3)_2\cdot 3H_2O$ (**3**), $[Cu_2(PAHAP)(gly)_2(NO_3)(H_2O)](NO_3)\cdot 3H_2O$ (**4**), $[Cu_2(PHMAP\text{-}H)(NO_3)_3(H_2O)(MeOH)]$ (**6**), $[Cu_2(PAHOX\text{-}H)_2](ClO_4)_2$ (**7**), and $[Cu(PAHOX)(SO_4)]_2\cdot 2H_2O$ (**8**). Complex **3** crystallized in the triclinic system, space group $P\bar{1}$ (No. 2), with $a = 17.503(4)$ Å, $b = 18.378(4)$ Å, $c = 10.742(4)$ Å, $\alpha = 93.44(3)°$, $\beta = 93.19(3)°$, $\gamma = 62.98(2)°$, and $Z = 4$. Complex **4** crystallized in the triclinic system, space group $P\bar{1}$, with $a = 11.506(12)$ Å, $b = 12.525(18)$ Å, $c = 10.319(4)$ Å, $\alpha = 94.47(7)°$, $\beta = 106.58(5)°$, $\gamma = 114.55(9)°$, and $Z = 2$. Complex **6** crystallized in the triclinic system, space group $P\bar{1}$, with $a = 7.4754(1)$ Å, $b = 8.7430(1)$ Å, $c = 17.9942(2)$ Å, $\alpha = 84.690(1)°$, $\beta = 83.190(1)°$, $\gamma = 66.885(1)°$, and $Z = 2$. Complex **7** crystallized in the monoclinic system, space group $C2/c$, with $a = 33.5849(6)$ Å, $b = 7.6016(1)$ Å, $c = 22.6654(3)$ Å, $\beta = 106.949(1)°$, and $Z = 8$. Complex **8** crystallized in the monoclinic system, space group $P2_1/n$, with $a = 9.866(2)$ Å, $b = 10.128(2)$ Å, $c = 15.418(1)$ Å, $\beta = 108.051(8)°$, and $Z = 4$. Antiferromagnetic exchange for **1**, **3**, **4**, and **6** ($-2J = 51.1$, 45.6, 1.5, and 208 cm^{-1}, respectively) is consistent with the angle of rotation (α) of the copper magnetic planes about the N−N bond. A linear relationship is found between α and $2J$ for a combined series of nine related complexes over an angle range of 105°. An estimate of the inherent ferromagnetism in the system is obtained from magnetic measurements close to the calculated angle of accidental orthogonality ($2J = 27$ cm^{-1}).

Introduction

N_2 diazine bridging ligands, e.g., pyrazoles, triazoles, pyridazines, and phthalazines, bring two metal centers into close proximity and provide an intramolecular pathway for spin-exchange interactions, which are exclusively antiferromagnetic in nature.[1−16] The N−N group has varying degrees of double bond character in these ligands, which is reflected in the extent of exchange coupling, but is rigidly fixed within the five- or six-membered diazine ring. The ligands PAHAP (picolinamide azine),[17] PMHAP,[18] and PHMAP (Figure 1a), which are derived from hydrazine and contain a single N−N bond, present several possible mononucleating and dinucleating coordination modes and, also, the potential for free rotation about the N−N bond. A related ligand (PAHOX, Figure 1a) involves a terminal oxime fragment, which can dominate the coordination mode of the

* Corresponding author. Fax: 709-737-3702. E-mail: lthomp@morgan.ucs.mun.ca.

† Memorial University.

‡ University of Durham.

(1) Kamiusuki, T.; Okawa, H.; Matsumoto, N.; Kida, S. *J. Chem. Soc., Dalton Trans.* **1990**, 195.
(2) Bayon, J. C.; Esteban, P.; Net, G.; Rasmussen, P. G.; Baker, K. N.; Hahn, C. W.; Gumz, M. M. *Inorg. Chem.* **1991**, *30*, 2572.
(3) Pons, J.; López, X.; Casabó, J.; Teixidor, F.; Caubet, A.; Ruis, J.; Miravitlles, C. *Inorg. Chim. Acta* **1992**, *195*, 61.
(4) Bencini, A.; Gatteschi, D.; Zanchini, C.; Haasnoot, J. G.; Prins, R.; Reedijk, J. *Inorg. Chem.* **1985**, *24*, 2812.
(5) Koomen-van Oudenniel, W. M. E.; de Graff, R. A. G.; Haasnoot, J. G.; Prins, R.; Reedijk, J. *Inorg. Chem.* **1989**, *28*, 1128.
(6) van Koningsbruggen, P. J.; Gatteschi, D.; de Graff, R. A. G.; Haasnoot, J. G.; Reedijk, J.; Zanchini, C. *Inorg. Chem.* **1995**, *34*, 5175.
(7) Prins, R.; Birker, P. J. M. W. L.; Haasnoot, J. G.; Verschoor, G. C.; Reedijk, J. *Inorg. Chem.* **1985**, *24*, 4128.
(8) Slangen, P. M.; van Koningsbruggen, P. J.; Haasnoot, J. G.; Jansen, J.; Gorter, S.; Reedijk, J.; Kooijman, H.; Smeets, W. J. J.; Spek, A. L. *Inorg. Chim. Acta* **1993**, *212*, 289.
(9) Abraham, F.; Lagrenee, M.; Sueur, S.; Mernari, B.; Brémard, C. *J. Chem., Soc., Dalton Trans*. **1991**, 1443.
(10) Mandal, S. K.; Thompson, L. K.; Newlands, M. J.; Lee, F. L.; LePage, Y.; Charland, J.-P.; Gabe, E. J. *Inorg. Chim. Acta* **1986**, *122*, 199.
(11) Thompson, L. K.; Mandal, S. K.; Charland, J.-P.; Gabe, E. J. *Can. J. Chem.* **1988**, *66*, 348.
(12) Tandon, S. S.; Thompson, L. K.; Hynes, R. C. *Inorg. Chem.* **1992**, *31*, 2210.
(13) Chen, L.; Thompson, L. K.; Bridson, J. N. *Inorg. Chem.* **1993**, *32*, 2938.
(14) Thompson, L. K.; Tandon, S. S.; Manuel, M. E. *Inorg. Chem.* **1995**, *34*, 2356.
(15) Tandon, S. S.; Thompson, L. K.; Manuel, M. E.; Bridson, J. N. *Inorg. Chem.* **1994**, *33*, 5555.
(16) van Koningsbruggen, P. J.; Haasnoot, J. G.; de Graff, R. A. G.; Reedijk, J.; Slingerland, S. *Acta Crystallogr.* **1992**, *C48*, 1923.
(17) Case, F. H. *J. Heterocycl. Chem.* **1970**, *7*, 1001.
(18) Xu. Z.; Thompson, L. K.; Miller, D. O. *Inorg. Chem.* **1997**, *36*, 3985.

S0020-1669(97)01519-X CCC: $15.00
Published on Web 05/30/1998

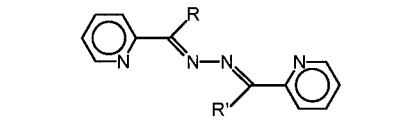

PAHAP (R=R'=NH_2); PMHAP (R=CH_3,R'=NH_2)

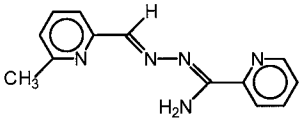

PHMAP

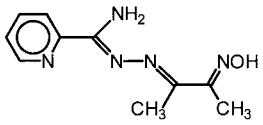

PAHOX

(a)

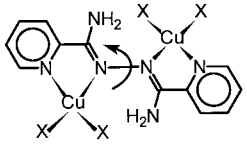

(b)

Figure 1. Diazine ligands and general bonding model.

ligand and generate NO-bridged dimers. In a recent paper, both PAHAP and PMHAP have been shown to coordinate to two copper(II) centers as N_4 donors, with a variety of geometrical arrangements which depend on coligands and reaction conditions (Figure 1b).[18] The complexes $[Cu_2(PAHAP)X_4]\cdot H_2O$ (X = Cl, Br) have pseudo-cis structures with dihedral angles between the copper planes of <80°, while, for the complexes $[Cu_2(PAHAP)(H_2O)_6](NO_3)_4$ and $[Cu_2(PMHAP\text{-}H)(NO_3)_3]$, much larger angles are observed (100.2° and 165.2° respectively).[18] The flexible geometries result from the ability of the systems to rotate freely about the single N−N bond of the diazine fragment of the ligands. PMHAP reaches its full coordination capacity by coordinating via all five nitrogens in $[Cu_2(PMHAP\text{-}H)(NO_3)_3]$, which effectively locks the complex into an almost flat trans structure. The magnetic properties of these two groups of compounds are very different, with the halide complexes exhibiting ferromagnetic coupling and the others antiferromagnetic exchange, with the antiferromagnetic contribution to exchange increasing with increasing dihedral angle. PAHAP, PMHAP, and PHMAP resemble the ligands PMK (bis(2-pyridylmethyl)ketazine)[19] and PAA (2-pyridine carbaldazine).[20−22] To our knowledge, there is only one structurally documented dicopper(II) complex of these ligands, $[Cu_2(PMK)Cl_4]$,[19] which has a folded square-planar *cis* conformation similar to that of $[Cu_2(PAHAP)X_4]\cdot H_2O$ (X = Cl, Br) (Figure 1b) and an acute angle between the copper planes (Cu−N−N−Cu torsion angle 70.8°). This complex exhibits weak antiferromagnetic coupling ($-2J$ = 52 cm^{-1}). A related complex with a fixed trans conformation, $[Cu_2(HL')Cl_3(H_2O)]\cdot 1.5H_2O$[23] ($H_2L'$ = bis(methyl-2-pyridyl ketone) carbonohydrazone), and an almost planar arrangement of two $d_{x^2-y^2}$ copper(II) centers with respect to the N−N bond also exhibits strong antiferromagnetic coupling ($-2J$ = 213.3 cm^{-1}). These results are in complete agreement with our previous study.[18] A cyclic tetranuclear copper(II) complex of the asymmetric hydrazone ligand *N,N′*-imidopicolinyloxamylhydrazine (L) $\{[Cu(L-H)]_4(NO_3)_4(H_2O)_8\}$[24] has a 90° twist between the copper square planes bound to each half of the ligand around the N−N bond, resulting in a negligible exchange interaction between the metal centers. A few other reports document the structures of dinuclear copper(II) complexes of hydrazone ligands with nominally single N−N bridges, but no variable-temperature magnetic data have been reported.[25−28]

In this report, structures are presented for $[Cu_2(PAHAP)(NCS)_4(DMF)_2]\cdot 2DMF$ (**1**), $[Cu_2(PAHAP)(bipy)_2(NO_3)_2](NO_3)_2\cdot 4H_2O$ (**2**) (details for **1** and **2** are preliminary because of poor refinement), $[Cu_2(PAHAP)(aln)_2(H_2O)_2](NO_3)_2\cdot 3H_2O$ (**3**) (aln = alaninate), $[Cu_2(PAHAP)(gly)_2(NO_3)(H_2O)](NO_3)\cdot 3H2O$ (**4**) (gly = glycinate), $[Cu_2(PHMAP\text{-}H)(NO_3)_3(H_2O)(MeOH)]$ (**6**), $[Cu_2(PAHOX\text{-}H)_2](ClO_4)_2$ (**7**), and the sulfato-bridged complex $[Cu(PAHOX)(SO_4)]_2\cdot 2H_2O$ (**8**). The cyanate complex $[Cu_2(PAHAP)(NCO)_4]\cdot 2DMF$ (**5**) is also reported. Variable-temperature magnetic measurements reveal anti-ferromagnetic behavior for **1** and **3**−**7** ($-2J$ = 51.1, 45.6, 1.5, 128, 208, and 549 cm^{-1}, respectively) and a noncoupled situation for **2** and **8**. These magnetic properties will be discussed in the light of the copper ion magnetic ground state, the torsional geometry with respect to the N−N bridge (**1**−**6**), the N−O bridge in **7**, and a μ_2-SO_4 bridge in **8**. These observations are supported by molecular orbital calculations at the extended Hückel level for the complexes themselves and, also, realistic models.

Experimental Section

Physical Measurements. Infrared spectra were recorded as Nujol mulls using a Mattson Polaris FT-IR instrument. UV/visible spectra were recorded in the solid state (mull transmittance and solution) using a Cary 5E spectrometer. Mass spectra were obtained using a VG Micromass 7070HS spectrometer. Microanalyses were carried out by Canadian Microanalytical Service, Delta, Canada. Room-temperature magnetic susceptibilities were measured by the Faraday method using a Cahn 7600 Faraday magnetic balance, and variable-temperature magnetic data (4−305 K) were obtained using an Oxford Instruments superconducting Faraday Susceptometer with a Sartorius 4432 microbalance. A main solenoid field of 1.5 T and a gradient field of 10 T m^{-1} were employed. The magnetic measurements were carried out on the same uniform samples that were analyzed structurally. $HgCo(NCS)_4$ was used as a calibration standard, and temperature errors were checked with the Curie−Weiss paramagnet $[TMENH_2][CuCl_4]$ (TMEN = $(CH_3)_2N(CH_2)_2N(CH_3)_2$).[29]

Synthesis of the Ligands. PHMAP. Picolinamide hydrazone[30] (13.6 g, 0.100 mol) was added to a boiling solution of 6′-methyl-2-pyridinecarboxaldehyde (12.1 g, 0.100 mol) in absolute ethanol (60 mL). The resulting solution was refluxed for 6 h. On cooling to room

(19) O'Connor, C. J.; Romananch, R. J.; Robertson, D. M.; Eduok, E. E.; Fronczek, F. R. *Inorg. Chem.* **1983**, *22*, 449.
(20) Stratton, W. J.; Busch, D. H. *J. Am. Chem. Soc.* **1958**, *80*, 1286.
(21) Stratton, W. J.; Busch, D. H. *J. Am. Chem. Soc.* **1960**, *82*, 4834.
(22) Ball, P. W.; Blake, A. B. *J. Chem. Soc. (A)* **1969**, 1415.
(23) Bacchi, A.; Bonini, A.; Carcelli, M.; Ferraro, F.; Leporati, E.; Pelizzi, C.; Pelizzi, G. *J. Chem. Soc. Dalton Trans.* **1996**, 2699.
(24) van Koningsbruggen, P. J.; Müller, E.; Haasnoot, J. G.; Reedijk, J. *Inorg. Chim. Acta* **1993**, *208*, 37.
(25) Koziol, A. E.; Palenik, R. C.; Palenik, G. J. *J. Chem. Soc., Chem. Commun.* **1989**, 650.
(26) Bachi, A.; Battaglia, L. P.; Carcelli, M.; Pelizzi, C.; Pelizzi, G.; Solinas, C.; Zoroddu, M. A. *J. Chem. Soc. Dalton Trans.* **1993**, 725.
(27) Lagrenée, M.; Sueur, S.; Wignacourt, J. P. *Acta Crystallogr.* **1991**, *C47*, 1158.
(28) Mangia, A.; Pelizzi, C.; Pelizzi, G. *Acta Crystallogr.* **1974**, *B30*, 2146.
(29) Brown, D. S.; Crawford, V. H.; Hall, J. W.; Hatfield, W. E. *J. Phys. Chem.* **1977**, *81*, 1303.
(30) Case, F. H. *J. Org. Chem.* **1965**, *30*, 931.

temperature, yellow crystals formed (yield 19 g, 80%, mp 125−126 °C). Mass spectrum (major mass peaks, *m*/*z*): 239 (M), 238 (M − H), 208, 147, 134, 119, 106, 79. IR: ν_{CN} 1618, 1604 cm^{-1}; ν_{NH} 3484, 3455, 3362, 3300 cm^{-1}. Anal. Calcd for $C_{13}H_{13}N_5$: C, 65.26; H, 5.48; N, 29.27. Found: C, 65.29; H, 5.46; N, 29.30.

PAHOX. 2,3-Butanedione monoxime (10.1 g, 0.100 mol) was dissolved in absolute ethanol (30 mL) and added slowly to a boiling solution of picolinamide hydrazone[30] (13.6 g, 0.100 mol) in absolute ethanol (40 mL). The resulting solution was refluxed for 4 h. Yellow crystals were obtained on cooling (yield 20 g, 92%). The product was recrystallized in high yield from hot ethanol (mp 153−155 °C). Mass spectrum (major mass peaks, *m*/*z*): 219 (M), 202, 161, 105, 98, 79, 78. IR: ν_{OH} 3470 cm^{-1}; ν_{NH} 3362, 3285 cm^{-1}; ν_{CN} 1610 cm^{-1}. Anal. Calcd for $C_{10}H_{13}N_5O$: C, 54.78; H, 5.98; N, 31.94. Found: C, 54.63; H, 5.98; N, 32.55.

Synthesis of the Complexes. $[Cu_2(PAHAP)(NCS)_4(DMF)_2]\cdot 2DMF$ (1) and $[Cu_2(PAHAP)(NCO)_4]\cdot 2DMF$ (5). $[Cu_2(PAHAP)(H_2O)_6](NO_3)_4$[18] (0.72 g, 1.00 mmol) was dissolved in water (40 mL) and added slowly with stirring to a solution of KSCN (0.58 g, 6.00 mmol) dissolved in water (30 mL). A yellow-green precipitate formed immediately, which was allowed to stand overnight, filtered, washed with deionized water, and dried under vacuum. Green crystals of **1** were obtained by diffusion of ether into a DMF/MeOH (1:1) solution of the solid (yield 0.90 g). Anal. Calcd for $[Cu_2(C_{12}H_{12}N_6)(NCS)_4(DMF)_2]\cdot 2DMF$ (**1**): C, 37.71; H, 4.52; N, 22.00. Found: C, 37.47; H, 4.37; N, 22.30. **5** was prepared in a similar fashion and recrystallized from DMF/MeOH to give a green crystalline powder. Anal. Calcd for $[Cu_2(C_{12}H_{12}N_6)(NCO)_4]\cdot 2DMF$ (**5**): C, 38.77; H, 3.84; N, 24.66. Found: C, 38.30; H, 3.19; N, 24.77.

$[Cu_2(PAHAP)(bipy)_2(NO_3)_2](NO_3)_2\cdot 4H_2O$ (2). Bipyridine (bipy) (0.312 g, 2.00 mmol) was added to a solution of $[Cu_2(PAHAP)(H_2O)_6](NO_3)_4$[18] (0.72 g, 1.00 mmol) dissolved in water (20 mL), forming a clear green solution after a few minutes. The solution was filtered and allowed to stand at room temperature for a few days. Deep green crystals formed, which were filtered off and dried in air (yield 0.60 g). Anal. Calcd for $[Cu_2(C_{12}H_{12}N_6)(bipy)_2(NO_3)_2]\ (NO_3)_2\cdot 4H_2O$ (**2**): C, 38.44; H, 3.63; N, 19.61. Found: C, 38.40; H, 3.35; N, 19.65.

$[Cu_2(PAHAP)(aln)_2(H_2O)_2](NO_3)_2\cdot 3H_2O$ (3) and $[Cu_2(PAHAP)(gly)_2(NO_3)(H_2O)]\ (NO_3)\cdot 3H_2O$ (4). *d*,*l*-Alanine (0.180 g, 2.0 mmol) was neutralized by addition of a solution of KOH (2.0 mmol in 5 mL of H_2O) and added to a solution of $[Cu_2(PAHAP)(H_2O)_6](NO_3)_4$[18] (0.724 g, 1.00 mmol) in water (15 mL), with the formation of a deep green solution. The solution was filtered and allowed to stand for 3 days. Dark blue, rodlike crystals formed, which were suitable for structural analysis (yield 0.80 g). Anal. Calcd for $[Cu_2(C_{12}H_{12}N_6)(C_3H_6NO_2)_2(NO_3)_2]\cdot 5H_2O$ (**3**): C, 28.54; H, 4.52; N, 18.49. Found: C, 28.26; H, 4.43; N, 18.39. **4** was prepared in a similar manner and obtained as green crystals. Anal. Calcd for $[Cu_2(C_{12}H_{12}N_6)(C_2H_4NO_2)(NO_3)_2]\cdot 4H_2O$ (**4**): C, 27.00; H, 3.97; N, 19.68. Found: C, 26.96; H, 3.83; N, 19.60.

$[Cu_2(PHMAP\text{-}H)(NO_3)_3(H_2O)(MeOH)]$ (6). PHMAP (0.24 g, 1.0 mmol) was dissolved in acetonitrile (10 mL) and added to a hot solution of $Cu(NO_3)_2\cdot 4H_2O$ (0.52 g, 2.0 mmol) in methanol (20 mL). The resulting dark green solution was filtered and the filtrate allowed to stand at room temperature overnight. Dark green, almost black crystals formed, which were filtered off, washed with methanol, and dried in air (yield 0.51 g). Anal. Calcd for $[Cu_2(C_{13}H_{12}N_5)(NO_3)_3(H_2O)(MeOH)]$ (**6**): C, 27.96; H, 3.02; N, 18.63. Found: C, 27.59; H, 2.95; N, 18.96.

$[Cu_2(PAHOX\text{-}H)_2](ClO_4)_2\cdot H_2O$ (7) and $[Cu(PAHOX)(SO_4)]_2\cdot 2H_2O$ (8). PAHOX (0.22 g, 1.0 mmol) was suspended in a solution of $Cu(ClO_4)_2\cdot 6H_2O$ (0.74 g, 2.0 mmol) in water (40 mL), and the mixture was heated to about 60 °C for a few minutes. A clear solution formed which was filtered and allowed to stand at room temperature for a few days. Dark, almost black crystals formed, which were filtered off and dried in air (yield 0.35 g). Anal. Calcd for $[Cu_2(C_{10}H_{12}N_5O)_2](ClO_4)_2\cdot H_2O$ (**7**): C, 30.78; H, 3.36; N,17.95. Found: C, 30.86; H, 3.25; N, 17.89. The analytical sample contains a water molecule that was not revealed in the structure. $[Cu(PAHOX)(SO_4)]_2\cdot 2H_2O$ (**8**) was prepared in a similar manner using $CuSO_4\cdot 5H_2O$ and obtained as dark green crystals. Anal. Calcd for $[Cu(C_{10}H_{13}N_5O)(SO_4)]_2\cdot 2H_2O$ (**8**): C, 30.26; H, 3.81; N, 17.65. Found: C, 30.39; H, 3.86; N, 17.80.

Crystallographic Data Collection and Refinement of the Structures. $[Cu_2(PAHOX\text{-}H)_2](ClO_4)_2$ (7). Crystals of **7** are dark green, almost black in appearance. A single crystal of **7** of dimensions 0.40 × 0.12 × 0.10 mm^3 was attached to a quartz fiber and transferred to a Siemens SMART 3-circle diffractometer with graphite-monochromatized Mo Kα X-radiation, and a CCD area detector was used for data collection.[31] ω-Scans were used in such a way that an initial 180° scan range consisting of 0.3° intervals was followed by three further 120°, 180°, and 120° scans with offsets of 88°, 180°, and 268°, respectively. This strategy samples the sphere of reciprocal space up to $2\theta = 50.04°$. Cell parameters were refined using the centroid values of 300 reflections with 2θ angles up to 50.04°. Raw frame data were integrated using the SAINT program.[32] The structure was solved by direct methods.[33a] An empirical absorption correction was applied to the data using the program SADABS.[34] H atoms bonded to C atoms were geometrically placed after each refinement cycle (C−H 0.95 Å, U(iso) = 1.2U(eq) for aromatic CH's; C−H 0.98 Å, U(iso) = 1.5U(eq) for CH_3 groups). H atoms bonded to N atoms were located from difference Fourier maps, and their coordinates and U(iso) values were refined.

Crystal data collection and structure refinement for **6** were carried out in a similar manner. H atoms bonded to C atoms were geometrically placed after each refinement cycle (C−H 0.95 Å, U(iso) = 1.2U(eq) for aromatic CH's; C−H 0.98 Å, U(iso) = 1.5U(eq) for CH_3 groups). H atoms bonded to N and O atoms were located from difference Fourier maps, and their coordinates and U(iso) values were refined. O(1)−H(11W) and O(1)−H(12W) distances were restrained to 0.85(1) Å. Abbreviated crystal data for **6** and **7** are given in Table 1 and significant atomic positional parameters in Tables 4 (**6**) and 5 (**7**). A full listing of experimental and crystal data for **6** and **7** is given in Table S1, and atomic positional parameters (Tables S4 and S5, respectively), anisotropic thermal parameters (Tables S9 and S10, respectively), and a full listing of bond distances and angles (Tables S12 and S13, respectively) are included as Supporting Information.

$[Cu(PAHOX)(SO_4)]_2\cdot 2H_2O$ (8). The crystals of **8** are green-yellow in appearance. The diffraction intensities of an approximately 0.20 × 0.20 × 0.40 mm^3 crystal were collected with graphite-monochromatized Mo Kα X-radiation using a Rigaku AFC6S diffractometer at 26 ± 1 °C and the $\omega-2\theta$ scan technique to a $2\theta_{max}$ value of 50.1°. A total of 2917 reflections was measured, and 1986 were considered significant, with $I_{net} > 2.0\sigma(I_{net})$. The intensities of three representative reflections, which were measured after every 150 reflections, remained constant throughout the data collection, indicating crystal and electronic stability (no decay correction was applied). Azimuthal scans of several reflections indicated no need for an absorption correction. The data were corrected for Lorentz and polarization effects. The cell parameters were obtained from the least-squares refinement of the setting angles of 20 carefully centered reflections with 2θ in the range 34.31−40.51°.

The structure was solved by direct methods.[35,36] All atoms except hydrogens were refined anisotropically. Hydrogen atoms were optimized by positional refinement, with isotropic thermal parameters set 20% greater than those of their bonded partners at the time of their inclusion. However, they were fixed for the final round of refinement. The final cycle of full-matrix least-squares refinement was based on 1986 observed reflections ($I > 2.00\sigma(I)$) and 209 variable parameters and converged with unweighted and weighted agreement factors of $\sum||F_o| - |F_c||/\sum|F_o| = 0.035$ and $R_w = [(\sum w(|F_o| - |F_c|)^2/\sum wF_o^2)]^{1/2}$

(31) Siemens. *SMART Data Collection Software*, Ver. 4.050; Siemens Analytical X-ray Instruments Inc.: Madison, WI, 1996.
(32) Siemens. *SAINT Data Reduction Software*, Version 4.050; Siemens Analytical X-ray Instruments Inc.: Madison, WI, 1996.
(33) (a) Sheldrick, G. M. *SHELXTL 5.04/VMS, An integrated system for solving, refining and displaying crystal structures from diffraction data;* Siemens Analytical X-ray Instruments Inc.: Madison, WI, 1995. (b) Sheldrick, G. M. *SHELX-97, A software package for the solution and refinement of X-ray data;* University of Göttingen: Göttingen, Germany, 1997.
(34) Sheldrick, G. M. SADABS, Empirical Absorption Correction Program; University of Göttingen: Göttingen, Germany, 1996.
(35) Gilmore, C. J. *J. Appl. Crystallogr.* **1984**, *17*, 42.
(36) Beurskens, P. T. *DIRDIF*; Technical Report 1984/1, Crystallography Laboratory, Toernooiveld, 6525 Ed Nijmegen, The Netherlands, 1984.

Table 1. Summary of Crystallographic Data for $[Cu_2(PAHAP)(aln)_2(H_2O)_2](NO_3)_2\cdot 3H_2O$ (**3**), $[Cu_2(PAHAP)(gly)_2(NO_3)(H_2O)](NO_3)\cdot 3H_2O$ (**4**) $[Cu_2(PHMAP\text{-}H)(NO_3)_3(H_2O)(MeOH)]$ (**6**), $[Cu_2(PAHOX\text{-}H)_2](ClO_4)_2$ (**7**), and $[Cu(PAHOX)(SO_4)]_2\cdot 2H_2O$ (**8**)

	3[a]	**4**[a]	**6**[b]	**7**[b]	**8**[a]
emp formula	$C_{18}H_{40}Cu_2N_{10}O_{15}$	$C_{16}H_{24}Cu_2N_{10}O_{12}$	$C_{14}H_{18}Cu_2N_8O_{11}$	$C_{20}H_{24}Cl_2Cu_2N_{10}O_{10}$	$C_{10}H_{15}CuN_5O_6S_6$
formula wt	763.66	675.53	601.44	762.47	396.86
space group	$P\bar{1}$	$P\bar{1}$	$P\bar{1}$	$C2/c$	$P2_1/n$ (No. 14)
a (Å)	17.503 (4)	11.506 (12)	7.4754 (1)	33.5849 (6)	9.866 (2)
b (Å)	18.378 (4)	12.525 (18)	8.7340 (1)	7.6016 (1)	10.128 (2)
c (Å)	10.742 (4)	10.319 (4)	17.9942 (2)	22.6654 (3)	15.418 (1)
α (deg)	93.44 (3)	94.47 (7)	84.690 (1)	90	90
β (deg)	93.19 (3)	106.58 (5)	83.190 (1)	106.949 (1)	108.051 (8)
γ (deg)	62.98 (2)	114.55 (9)	66.885 (1)	90	90
V (Å^3)	3071 (2)	1263 (2)	1071.54 (2)	5535.1 (1)	1464.7 (3)
ρ_{calcd} (g cm^{-3})	1.652	1.776	1.864	1.830	1.800
Z	4	2	2	8	4
μ	1.469 mm^{-1}	1.765 mm^{-1}	2.062 mm^{-1}	1.804 mm^{-1}	16.68 cm^{-1}
λ (Å)	0.710 69	0.710 69	0.710 73	0.710 73	0.710 69
T (K)	299 (2)	299 (2)	150 (2)	150 (2)	299 (1)
$R1$ (R)[c]	0.060 (R)	0.0538	0.0483	0.0465	0.035 (R)
w$R2$ (R_w)[c]	0.048 (R_w)	0.1257	0.1038	0.0753	0.033 (R_w)

[a] Rigaku data. [b] Siemens Smart data. [c] $R_1 = \sum||F_o| - |F_c||/\sum|F_o|$, $wR_2 = [\sum[w(|F_o|^2 - |F_c|^2)^2]/\sum[w(|F_o|^2)^2]]^{1/2}$. $R = \sum||F_o| - |F_c||/\sum|F_o|$, $R_w = [(\sum w(|F_o| - |F_c|)^2/\sum wF_o^2)]^{1/2}$.

Table 2. Final Atomic Positional Parameters and B(eq) for Significant Atoms in $[Cu_2(PAHAP)(aln)_2(H_2O)_2](NO_3)_2\cdot 3H_2O$ (**3**)

atom	x	y	z	B (eq)[a]	atom	x	y	z	B (eq)[a]
Cu(1)	0.15346(4)	0.28979(4)	0.64009(5)	2.76(1)	N(12)	0.7202(2)	0.2557(2)	0.9250(3)	2.16(7)
Cu(2)	0.39555(4)	0.06327(4)	0.62115(5)	2.56(1)	N(13)	0.6321(2)	0.2554(3)	1.0804(3)	4.2(1)
Cu(3)	0.59930(4)	0.43538(4)	0.89280(5)	2.72(1)	N(14)	0.8593(2)	0.1558(2)	1.0383(3)	2.72(8)
Cu(4)	0.84156(4)	0.21037(4)	0.87676(5)	2.96(1)	N(15)	0.6821(2)	0.4393(2)	1.0209(3)	2.89(9)
O(1)	0.0310(2)	0.3437(2)	0.6643(3)	3.46(8)	N(16)	0.8273(2)	0.2470(2)	0.7041(3)	3.63(9)
O(2)	−0.0688(2)	0.3718(2)	0.8005(3)	6.2(1)	N(17)	0.8155(3)	0.0299(3)	0.8527(5)	4.7(1)
O(3)	0.4636(2)	−0.0499(2)	0.5609(3)	2.79(7)	N(18)	0.1805(3)	0.4717(4)	0.6749(6)	6.2(1)
O(4)	0.4577(2)	−0.1447(2)	0.4295(3)	3.32(8)	N(19)	0.6531(4)	0.2836(4)	0.4427(6)	7.3(2)
O(5)	0.1393(2)	0.1765(2)	0.5318(3)	3.29(9)	N(20)	0.2619(6)	0.2102(6)	0.1211(8)	8.4(3)
O(6)	0.3294(2)	0.0150(2)	0.7530(3)	4.62(9)	N(21)	0.3518(6)	0.2079(7)	0.1593(8)	8.6(3)
O(7)	0.5340(2)	0.5522(2)	0.9348(3)	2.82(7)	C(1)	0.0691(3)	0.3964(3)	0.4256(4)	3.4(1)
O(8)	0.5468(2)	0.6572(2)	1.0252(3)	4.32(8)	C(2)	0.0674(3)	0.4370(3)	0.3206(4)	3.6(1)
O(9)	0.9626(2)	0.1566(2)	0.8399(3)	3.55(8)	C(3)	0.1427(3)	0.4237(3)	0.2708(4)	3.7(1)
O(10)	1.0550(2)	0.1294(2)	0.6922(3)	5.7(1)	C(4)	0.2193(3)	0.3678(3)	0.3268(4)	3.1(1)
O(11)	0.6639(3)	0.4686(3)	0.7173(4)	8.5(1)	C(5)	0.2164(3)	0.3281(3)	0.4307(4)	2.3(1)
O(12)	0.8597(2)	0.3246(2)	0.9709(3)	3.51(9)	C(6)	0.2931(3)	0.2670(3)	0.4990(4)	2.19(9)
O(13)	0.8409(3)	0.0662(2)	0.7877(4)	6.0(1)	C(7)	0.3845(3)	0.2049(3)	0.7539(4)	2.39(9)
O(14)	0.8626(3)	−0.0428(2)	0.8823(4)	6.9(1)	C(8)	0.4571(3)	0.1353(3)	0.8161(4)	2.46(9)
O(15)	0.7418(2)	0.0652(2)	0.8928(4)	6.8(1)	C(9)	0.5050(3)	0.1449(3)	0.9170(4)	3.1(1)
O(16)	0.2544(3)	0.4331(3)	0.6484(4)	7.8(1)	C(10)	0.5714(3)	0.0746(3)	0.9661(4)	3.3(1)
O(17)	0.1540(3)	0.4362(3)	0.7413(5)	9.9(2)	C(11)	0.5876(3)	−0.0004(3)	0.9144(4)	3.2(1)
O(18)	0.1345(3)	0.5362(3)	0.6313(5)	8.8(2)	C(12)	0.5373(3)	−0.0048(3)	0.8138(4)	2.9(1)
O(19)	0.6846(3)	0.3202(3)	0.5072(5)	11.2(2)	C(13)	0.0076(3)	0.3444(3)	0.7743(5)	4.0(1)
O(20)	0.6678(4)	0.2174(3)	0.4721(4)	11.6(2)	C(14)	0.0783(4)	0.3099(4)	0.8742(6)	6.7(2)
O(21)	0.6114(4)	0.3116(3)	0.3488(4)	11.2(2)	C(15)	0.0720(5)	0.3619(7)	0.9687(8)	19.9(4)
O(22)	0.1893(6)	0.2152(7)	0.1169(8)	9.4(3)	C(16)	0.4253(3)	−0.0742(3)	0.4767(4)	2.50(9)
O(23)	0.3009(3)	0.2280(3)	0.0504(4)	10.1(2)	C(17)	0.3369(3)	−0.0144(3)	0.4296(5)	3.7(1)
O(24)	0.2932(3)	0.1795(3)	0.2199(4)	8.3(1)	C(18)	0.2685(3)	−0.0326(3)	0.4589(6)	6.9(2)
O(25)	0.4105(4)	0.2408(5)	0.1884(5)	7.8(2)	C(19)	0.4586(3)	0.4950(3)	0.7021(4)	3.6(1)
O(26)	0.9303(3)	0.3123(3)	0.2173(4)	8.8(1)	C(20)	0.4095(3)	0.4866(3)	0.6016(5)	4.5(1)
O(27)	0.7531(3)	0.3455(3)	0.2501(5)	2.9(1)	C(21)	0.4246(3)	0.4095(3)	0.5588(5)	4.6(1)
O(28)	0.5883(2)	0.1600(2)	0.2726(3)	6.28(9)	C(22)	0.4888(3)	0.3428(3)	0.6167(4)	3.5(1)
O(29)	0.4308(4)	0.3446(4)	0.2695(6)	5.2(2)	C(23)	0.5350(3)	0.3554(3)	0.7149(4)	2.50(9)
O(30)	0.0958(3)	0.1822(3)	0.2746(4)	8.8(1)	C(24)	0.6076(3)	0.2900(3)	0.7823(4)	2.32(9)
O(31)	0.1784(2)	0.0865(2)	0.8733(3)	6.3(1)	C(25)	0.7074(3)	0.2317(3)	1.0303(4)	2.5(1)
O(32)	0.8122(3)	0.4262(3)	0.6080(4)	8.0(1)	C(26)	0.7863(3)	0.1712(3)	1.0961(4)	2.7(1)
N(1)	0.1423(2)	0.3425(2)	0.4788(3)	2.41(8)	C(27)	0.7867(3)	0.1320(3)	1.2010(4)	3.8(1)
N(2)	0.3707(2)	0.2408(2)	0.4543(3)	3.08(9)	C(28)	0.8654(4)	0.0753(3)	1.2486(4)	4.2(1)
N(3)	0.2760(2)	0.2452(2)	0.6023(3)	2.28(7)	C(29)	0.9403(3)	0.0602(3)	1.1918(5)	4.3(1)
N(4)	0.3472(2)	0.1818(2)	0.6624(3)	2.44(8)	C(30)	0.9347(3)	0.1017(3)	1.0862(4)	3.5(1)
N(5)	0.3639(2)	0.2816(2)	0.7894(3)	3.59(9)	C(31)	0.5770(3)	0.5826(3)	0.9979(4)	2.7(1)
N(6)	0.4745(2)	0.0611(2)	0.7636(3)	2.38(8)	C(32)	0.6671(3)	0.5254(3)	1.0440(5)	4.0(1)
N(7)	0.1606(2)	0.2584(2)	0.8180(3)	3.39(9)	C(33)	0.7316(3)	0.5429(4)	0.9905(7)	7.7(2)
N(8)	0.3213(2)	0.0700(2)	0.4723(3)	2.72(8)	C(34)	0.9810(3)	0.1592(3)	0.7297(5)	3.7(1)
N(9)	0.5195(2)	0.4316(2)	0.7586(3)	2.56(8)	C(35)	0.9053(4)	0.1941(4)	0.6360(5)	6.5(1)
N(10)	0.6281(2)	0.2121(2)	0.7565(3)	3.20(9)	C(36)	0.9088(5)	0.1732(9)	0.5292(7)	31.6(5)
N(11)	0.6476(2)	0.3157(2)	0.8655(3)	2.26(7)					

[a] $B_{(eq)} = (8\pi^2/3)\sum_{i=1}^{3}\sum_{j=1}^{3}U_{ij}a_ia_j\vec{a}_i\cdot\vec{a}_j$.

Table 3. Final Atomic Coordinates ($\times 10^4$) and Equivalent Isotropic Displacement Parameters ($Å^2 \times 10^3$) for Significant Atoms in $[Cu_2(PAHAP)(gly)_2(NO_3)(H_2O)](NO_3)\cdot 3H_2O$ (**4**)

atom	*x*	*y*	*z*	*U*(eq)[a]
Cu(1)	10085(1)	738(1)	6716(1)	30(1)
Cu(2)	9189(1)	3392(1)	8741(1)	26(1)
N(1)	12085(5)	1360(5)	7446(5)	30(1)
N(2)	10640(5)	2477(4)	7250(5)	25(1)
N(3)	12511(5)	4392(5)	7964(5)	34(1)
N(4)	9575(6)	3120(5)	4896(5)	39(1)
N(5)	9788(5)	3028(5)	7212(5)	26(1)
N(6)	8115(5)	3883(5)	7257(5)	28(1)
C(1)	12752(7)	700(7)	7663(7)	42(2)
C(2)	14121(8)	1185(7)	8318(9)	51(2)
C(3)	14858(8)	2398(8)	8726(8)	49(2)
C(4)	14210(7)	3120(7)	8488(7)	37(2)
C(5)	12815(6)	2568(6)	7867(6)	27(1)
C(6)	11942(6)	3202(5)	7675(5)	25(1)
C(7)	9265(6)	3256(6)	6017(6)	28(1)
C(8)	8267(6)	3717(5)	6012(6)	27(1)
C(9)	7523(7)	3958(7)	4869(6)	40(2)
C(10)	6609(8)	4372(7)	5000(7)	46(2)
C(11)	6458(7)	4532(7)	6265(7)	44(2)
C(12)	7224(7)	4280(6)	7362(6)	33(2)
O(1)	9719(5)	−875(4)	5946(4)	36(1)
O(2)	8113(5)	−2776(4)	5307(5)	41(1)
N(7)	8091(5)	54(5)	6205(6)	43(2)
C(13)	7496(7)	−1269(6)	5944(8)	41(2)
C(14)	8497(7)	−1704(6)	5704(6)	31(2)
O(3)	8741(5)	4041(4)	10222(4)	35(1)
O(4)	8766(4)	3960(4)	12365(4)	37(1)
N(8)	10244(5)	2895(5)	10220(5)	32(1)
C(15)	9785(8)	2943(6)	11425(6)	38(2)
C(16)	9047(6)	3704(6)	11349(6)	27(1)
N(20)	3758(8)	3252(6)	1325(6)	50(2)
O(21)	2813(7)	2277(6)	1094(8)	91(2)
O(22)	4931(7)	3484(9)	1786(7)	113(3)
O(23)	3441(9)	4064(6)	972(7)	93(2)
N(30)	10000	0	10000	63(3)
O(31)	9746(13)	446(10)	9022(10)	50(3)
O(32)	10220(16)	−177(14)	8966(13)	74(4)
O(33)	9067(14)	375(11)	9920(2)	101(6)
O(50)	7244(7)	1483(6)	8144(7)	89(2)
N(40)	5000	0	5000	128(13)
O(41)	4360(10)	−30(12)	5770(4)	280(4)
O(42)	5880(5)	750(3)	4600(7)	190(3)
O(43)	5310(3)	990(2)	5610(4)	114(10)
O(60)	15170(3)	−1074(16)	8047(18)	204(10)
O(70)	6850(3)	−110(2)	9420(3)	128(10)

[a] *U*(eq) is defined as one-third the trace of the orthogonalized U_{ij} tensor.

= 0.033. The maximum and minimum peaks on the final difference Fourier map correspond to 0.39 and −0.45 electrons $Å^{-3}$ respectively. Neutral atom scattering factors[37] and anomalous dispersion terms[38,39] were taken from the usual sources. All calculations were performed with the TEXSAN[40] crystallographic software package using a VAX 3100 work station. Crystal data collection and structure refinement for **3** were carried out in a similar manner. The data for **4** were collected as for **3**, a ψ-scan absorption correction being applied. The structure was solved by direct methods and refined on F^2 using the SHELX-97 package running on DOS 6.22.[33b] Abbreviated crystal data are given in Table 1, and significant atomic positional parameters are given in Tables 2 (**3**), 3 (**4**) and 6 (**8**). A full listing of experimental and crystal data (Table S1), full listings of atomic positional parameters (Tables S2, S3, and S6, respectively), anisotropic thermal parameters (Tables S7, S8, and S11, respectively), and full listings of bond distances and angles (Tables S12, S13, and S16, respectively) are included as Supporting Information.

Table 4. Final Atomic Coordinates ($\times 10^4$) and Equivalent Isotropic Displacement Parameters ($Å^2 \times 10^3$) for Significant Atoms in $[Cu_2(PHMAP\text{-}H)(NO_3)_3(H_2O)(MeOH)]$ (**6**)

atom	*x*	*y*	*z*	*U*(eq)[a]
Cu(1)	−3829(1)	11927(1)	3222(1)	28(1)
Cu(2)	−8609(1)	16626(1)	2061(1)	26(1)
C(1)	−4854(7)	12130(5)	4894(2)	32(1)
C(2)	−5849(7)	12926(5)	5537(2)	34(1)
C(3)	−7308(6)	14494(5)	5474(2)	32(1)
C(4)	−7732(6)	15230(5)	4765(2)	26(1)
C(5)	−6710(5)	14360(5)	4146(2)	22(1)
C(6)	−7128(5)	14981(4)	3356(2)	20(1)
C(7)	−5993(6)	13547(5)	1563(2)	24(1)
C(8)	−6895(5)	14436(5)	880(2)	20(1)
C(9)	−9259(6)	16865(5)	384(2)	24(1)
C(10)	−8712(6)	16243(5)	−332(2)	28(1)
C(11)	−7241(6)	14688(5)	−429(2)	29(1)
C(12)	−6334(6)	13748(5)	186(2)	25(1)
C(13)	−10933(6)	18502(5)	518(2)	32(1)
C(14)	−6506(10)	10259(8)	3001(4)	67(2)
N(1)	−5277(5)	12831(4)	4206(2)	26(1)
N(2)	−8364(6)	16410(5)	3143(2)	28(1)
N(3)	−6067(5)	13799(4)	2854(2)	23(1)
N(4)	−6620(4)	14386(4)	2151(2)	20(1)
N(5)	−8325(5)	15984(4)	978(2)	23(1)
N(7)	−7666(5)	19406(4)	1503(2)	27(1)
N(8)	−12189(5)	15995(4)	2400(2)	26(1)
O(1)	−2089(4)	12010(4)	2293(2)	28(1)
O(2)	−4736(6)	10135(5)	2808(2)	51(1)
O(6)	−9083(4)	19105(3)	1903(1)	26(1)
O(7)	−7870(5)	20859(4)	1348(2)	43(1)
O(8)	−6192(5)	18205(4)	1288(2)	45(1)
O(9)	−11802(4)	17301(3)	2268(2)	26(1)
O(10)	−10908(5)	14643(4)	2184(2)	43(1)
O(11)	−13760(5)	16083(4)	2722(2)	42(1)
O(31)	−1821(16)	9959(11)	3677(6)	36(2)
N(61)	−585(9)	10356(6)	3986(3)	32(1)
O(41)	−787(7)	11837(6)	3973(3)	39(1)
O(51)	756(7)	9198(5)	4282(2)	43(1)
O(32)	−1466(66)	10247(43)	3673(25)	36(2)
N(62)	99(29)	10695(22)	3750(10)	32(1)
O(42)	−184(25)	12144(22)	3692(10)	39(1)
O(52)	1647(23)	9589(17)	3906(8)	43(1)

[a] *U*(eq) is defined as one-third of the trace of the orthogonalized U_{ij} tensor.

Results and Discussion

Structures. $[Cu_2(PAHAP)(NCS)_4(DMF)_2]\cdot 2.16H_2O$ (1). The preliminary structural representation of **1** is illustrated in Figure 2. The dinuclear complex has a twisted structure, with the two copper(II) square pyramids bridged by the N−N diazine unit. Two isothiocyanates are bound in positions cis to the copper basal planes, with two PAHAP nitrogens occupying the other basal sites. The NH_2 groups on PAHAP remain uncoordinated. Equatorial Cu−N distances are quite short (<2.03 Å), with somewhat longer contacts to axial DMF molecules (Cu(2)−O(2) 2.337(5) Å, Cu(1)−O(1) 2.229(5) Å). Some positional disorder was observed for S13, and it has been modeled with two 50% site occupancies. The copper centers are separated by 4.453 Å, and the two copper planes are twisted about the N−N bond by a dihedral angle of 103.6° (angle between the least-squares planes defined by Cu(1)−N(1)−C(5)−C(6)−N(2) and Cu(2)−N(4)−C(11)−C(12)−N(5)).

$[Cu_2(PAHAP)(bipy)_2(NO_3)_2](NO_3)_2\cdot 4H_2O$ (2). The preliminary structural representation of the cationic fragment of **2**

(37) Cromer, D. T.; Waber, J. T. *International Tables for X-ray Crystallography*; The Kynoch Press: Birmingham, U.K., 1974; Vol. IV, Table 2.2A.
(38) Ibers, J. A.; Hamilton, W. C. *Acta Crystallogr.* **1974**, *17*, 781.
(39) Cromer, D. T. *International Tables for X-ray Crystallography*; The Kynoch Press: Birmingham, U.K., 1974; Vol. IV, Table 2.3.1.
(40) *Texsan−Texray Structure Analysis Package*; Molecular Structure Corp.: The Woodlands, TX, 1985.

Table 5. Final Atomic Coordinates ($\times 10^4$) and Equivalent Isotropic Displacement Parameters ($Å^2 \times 10^3$) for Significant Atoms in $[Cu_2(PAHOX\text{-}H)_2](ClO_4)_2$ (**7**)

atom	*x*	*y*	*z*	*U*(eq)[a]
Cu(1)	1809(1)	6025(1)	786(1)	17(1)
Cu(2)	736(1)	6709(1)	239(1)	18(1)
C(1)	2127(1)	7288(5)	2107(2)	24(1)
C(2)	2435(1)	7731(5)	2642(2)	26(1)
C(3)	2846(1)	7681(5)	2647(2)	26(1)
C(4)	2940(1)	7203(4)	2111(2)	24(1)
C(5)	2619(1)	6743(4)	1598(1)	18(1)
C(6)	2673(1)	6137(4)	1003(1)	17(1)
C(7)	2080(1)	4670(4)	−412(2)	19(1)
C(8)	2199(1)	3824(5)	−937(2)	24(1)
C(9)	1632(1)	5009(4)	−507(2)	19(1)
C(10)	1327(1)	4744(5)	−1133(2)	31(1)
C(11)	561(1)	8827(5)	−935(2)	23(1)
C(12)	311(1)	9807(5)	−1417(2)	26(1)
C(13)	−104(1)	10034(5)	−1456(2)	26(1)
C(14)	−261(1)	9267(4)	−1014(2)	23(1)
C(15)	7(1)	8342(4)	−540(2)	19(1)
C(16)	−108(1)	7502(4)	−21(2)	19(1)
C(17)	360(1)	5398(4)	1347(2)	19(1)
C(18)	187(1)	4758(5)	1853(2)	30(1)
C(19)	816(1)	5248(4)	1459(2)	19(1)
C(20)	1078(1)	4450(5)	2049(2)	28(1)
N(1)	2216(1)	6764(4)	1597(1)	20(1)
N(2)	3047(1)	6025(4)	923(2)	23(1)
N(3)	2324(1)	5724(3)	578(1)	18(1)
N(4)	2394(1)	5006(4)	55(1)	19(1)
N(5)	1492(1)	5556(3)	−60(1)	18(1)
N(6)	414(1)	8113(3)	−502(1)	19(1)
N(7)	−497(1)	7520(5)	2(2)	25(1)
N(8)	202(1)	6769(4)	401(1)	19(1)
N(9)	79(1)	6052(4)	882(1)	22(1)
N(10)	998(1)	5780(4)	1052(1)	18(1)
O(1)	1080(1)	5862(3)	−228(1)	26(1)
O(2)	1411(1)	5617(3)	1228(1)	23(1)

[a] *U*(eq) is defined as one-third of the trace of the orthogonalized U_{ij} tensor.

Table 6. Final Atomic Positional Parameters and *B*(eq) for Significant Atoms in $[Cu(PAHOX)(SO_4)]_2 \cdot 2H_2O$ (**8**)

atom	*x*	*y*	*z*	*B*(eq)[a]
Cu(1)	0.18766(5)	0.15861(5)	0.48906(3)	2.11(2)
S(1)	0.0506(1)	−0.1124(1)	0.39428(7)	2.10(4)
O(1)	0.3700(3)	−0.0691(3)	0.5639(2)	3.6(1)
O(2)	0.1234(3)	0.0173(3)	0.3975(2)	2.4(1)
O(3)	0.0326(3)	−0.1735(3)	0.3061(2)	3.3(1)
O(4)	0.1438(3)	−0.1946(3)	0.4677(2)	3.1(1)
O(5)	−0.0873(3)	−0.0927(3)	0.4095(2)	2.7(1)
N(1)	0.0394(3)	0.2788(3)	0.4110(2)	2.2(1)
N(2)	0.2833(3)	0.3250(3)	0.5283(2)	2.3(1)
N(3)	0.4130(3)	0.3546(3)	0.5907(2)	2.7(1)
N(4)	0.3659(3)	0.0675(3)	0.5648(2)	2.3(1)
N(5)	0.2720(4)	0.5517(3)	0.5005(2)	3.1(2)
C(1)	−0.0868(4)	0.2439(4)	0.3536(3)	2.7(2)
C(2)	−0.1813(4)	0.3352(5)	0.3015(3)	3.3(2)
C(3)	−0.1443(5)	0.4665(5)	0.3108(3)	3.7(2)
C(4)	−0.0146(5)	0.5038(4)	0.3705(3)	3.2(2)
C(5)	0.0752(4)	0.4086(4)	0.4198(3)	2.2(2)
C(6)	0.2178(4)	0.4317(4)	0.4865(3)	2.1(2)
C(7)	0.4989(4)	0.2623(4)	0.6306(3)	2.5(2)
C(8)	0.4799(4)	0.1179(4)	0.6197(3)	2.2(2)
C(9)	0.6342(4)	0.3116(5)	0.6965(3)	3.8(2)
C(10)	0.5975(4)	0.0307(5)	0.6733(3)	3.6(2)

[a] $B(\text{eq}) = (8\pi^2/3)\sum_{i=1}^{3}\sum_{j=1}^{3} U_{ij} a_i a_j \vec{a}_i \cdot \vec{a}_j$.

is illustrated in Figure 3. The dinuclear complex involves two distorted five-coordinate copper(II) centers, each with two PAHAP nitrogens (pyridine and diazine), two bipyridine nitrogens, and a terminal nitrate ligand. The bidentate bipy ligands

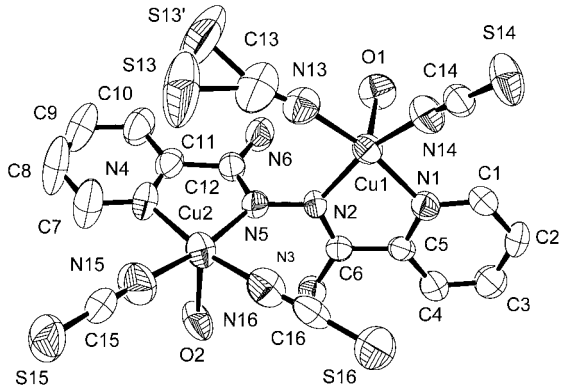

Figure 2. Structural representation for **1**, with hydrogen atoms omitted (50% probability thermal ellipsoids). Preliminary Siemens Smart data: $C_{22}H_{30.32}Cu_2N_{12}O_{4.16}S_4$; space group *C*2/*c*, $a = 36.7978(9)$ Å, $b = 15.7510(3)$ Å, $c = 16.1358(4)$ Å, $\alpha = 90.0°$, $\beta = 114.992(1)°$, $\gamma = 90.0°$, $V = 8476.7(3)$ Å^3, $Z = 8$, $\lambda = 0.710\ 73$ Å.

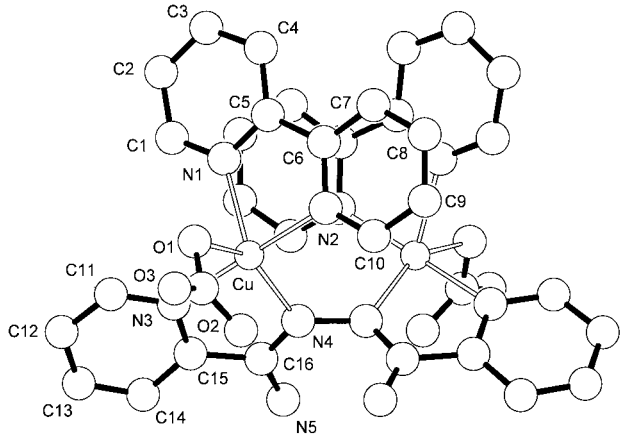

Figure 3. Structural representation for **2**, with hydrogen atoms omitted (50% probability thermal ellipsoids). Preliminary Siemens Smart data: $C_{32}H_{28}Cu_2N_{12}O_6$; space group *Pcca*, $a = 13.9286(8)$ Å, $b = 12.5106(8)$ Å, $c = 24.578(1)$ Å, $\alpha = 90.0°$, $\beta = 90.0°$, $\gamma = 90.0°$, V=4282.8(4) Å^3, Z = 4, $\lambda = 0.710\ 73$ Å.

have short copper−nitrogen distances, with Cu−N(1) (2.132(5) Å) slightly longer than Cu−N(2) (1.998(5) Å). The copper ion geometry is between a square pyramid and a trigonal bipyramid, and, using the distortion index established by Addison et al.[41] ($\tau = (\beta - \alpha)/60$; $\beta = 179.0°$, $\alpha = 144.3°$), a value of 0.58 suggests that a distorted trigonal bipyramid is the most appropriate stereochemical description. The axial direction would then be defined by N(2)−Cu−N(3). The molecular twist around the N−N bond is much more pronounced, with a much larger dihedral angle (119.8°) between the $Cu-N_{diazine}-N_{pyridine}$ planes (as indicated by the angle between the Cu−N(3)−C(15)−C(16)−N(4) plane and the symmetry-related least-squares plane). This results because there is a major steric effect between the two bipy ligands, and they align themselves roughly parallel, effectively twisting the two copper planes about the N−N bond in an attempt to keep the planar bipy ligands a safe distance from each other. The relatively large twist angle around the N−N bond leads to quite a large Cu−Cu separation (4.229 Å), when compared with that in $[Cu_2(PAHAP)Cl_4]\cdot H_2O$.[18]

$[Cu_2(PAHAP)(aln)_2(H_2O)_2](NO_3)_2\cdot 3H_2O$ (3). The structure of one of the two crystallographically independent, but very similar, molecules in **3** is illustrated in Figure 4, and bond

(41) Addison, A. W.; Rao, T. N.; Reedijk, J.; van Rijn, J.; Verschoor, G. C. *J. Chem. Soc., Dalton Trans.* **1984**, 1349.

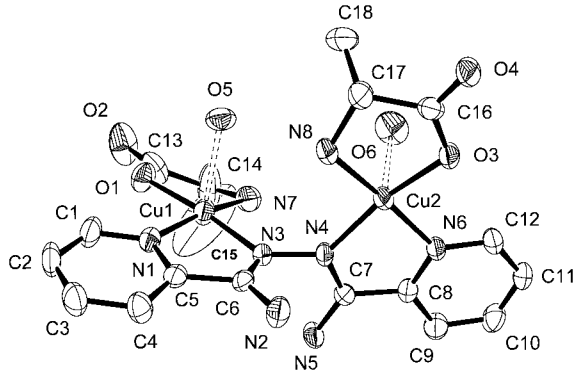

Figure 4. Structural representation for **3** with hydrogen atoms omitted (50% probability thermal ellipsoids).

Table 7. Interatomic Distances (Å) and Angles (Deg) Relevant to the Copper Coordination Spheres in $[Cu_2(PAHAP)(aln)_2(H_2O)_2](NO_3)_2\cdot 3H_2O$ (**3**)

Cu(1)−O(1)	1.936(3)	Cu(3)−O(11)	2.492(5)
Cu(1)−N(1)	1.993(4)	Cu(3)−N(9)	1.972(4)
Cu(1)−N(3)	1.973(4)	Cu(3)−N(11)	1.975(4)
Cu(1)−N(7)	2.010(4)	Cu(3)−N(15)	1.965(4)
Cu(1)−O(5)	2.428(4)	Cu(3)−O(7)	2.979(4)
Cu(2)−O(3)	1.959(3)	Cu(4)−O(9)	1.940(3)
Cu(2)−N(4)	1.977(4)	Cu(4)−N(12)	1.984(4)
Cu(2)−N(6)	1.994(4)	Cu(4)−N(14)	1.995(4)
Cu(2)−N(8)	1.977(4)	Cu(4)−N(16)	1.975(4)
Cu(2)−O(6)	2.325(4)	Cu(4)−O(12)	2.417(4)
Cu(3)−O(7)	1.957(3)	Cu(4)−O(13)	2.767(5)
Cu(1)−Cu(2)	4.392(4)	Cu(3)−Cu(4)	4.379(4)
N(3)−N(4)	1.418(4)	N(11)−N(12)	1.400(4)

O(1)−Cu(1)−N(1)	93.3(1)	O(7)−Cu(3)−N(9)	95.9(1)
O(1)−Cu(1)−N(3)	173.3(2)	O(7)−Cu(3)−N(11)	169.2(2)
O(1)−Cu(1)−N(7)	84.1(1)	O(7)−Cu(3)−N(15)	84.5(1)
N(1)−Cu(1)−N(3)	80.5(1)	O(11)−Cu(3)−N(9)	82.3(2)
N(1)−Cu(1)−N(7)	168.6(2)	O(11)−Cu(3)−N(11)	100.1(2)
N(3)−Cu(1)−N(7)	101.4(2)	O(11)−Cu(3)−N(15)	95.3(2)
O(3)−Cu(2)−N(4)	166.6(2)	N(9)−Cu(3)−N(11)	80.9(1)
O(3)−Cu(2)−N(6)	96.7(1)	N(9)−Cu(3)−N(15)	177.5(2)
O(3)−Cu(2)−N(8)	84.2(1)	N(11)−Cu(3)−N(15)	99.1(1)
N(4)−Cu(2)−N(6)	80.6(1)	O(9)−Cu(4)−N(12)	174.2(2)
N(4)−Cu(2)−N(8)	97.5(1)	O(9)−Cu(4)−N(14)	93.9(1)
N(6)−Cu(2)−N(8)	175.3(2)	O(9)−Cu(4)−N(16)	83.7(1)
O(7)−Cu(3)−O(11)	89.6(1)	N(12)−Cu(4)−N(14)	80.9(1)

distances and angles relevant to the copper coordination spheres are given in Table 7. The copper(II) centers are close to square pyramidal, with short equatorial contacts (<2.0 Å) to an N_3O in-plane donor set and weak axial coordination by two water molecules (e.g., Cu(1)−O(5) 2.428(4), Cu(2)−O(6) 2.325(4) Å, Cu(3)−O(11) 2.492(5) Å, Cu(4)−O(12) 2.417(4) Å). The copper basal planes are twisted about the diazine N−N bond, with twist angles of 85.9(4)° between the least-squares planes Cu(1)−N(1)−C(5)−C(6)−N(3) and Cu(2)−N(4)−C(7)−C(8)−N(6) (torsion angle Cu(1)−N(3)−N(4)−Cu(2) 87.8(4)°) and 89.1(4) between the least-squares planes Cu(3)−N(9)−C(23)−C(24)−N(11) and Cu(4)−N(12)−C(25)−C(26)−N(14) (torsion angle Cu(3)−N(11)−N(12)−Cu(4) 86.8(4)°). The copper atoms are separated by 4.392(4) (Cu(1)−Cu(2)) and 4.379(4) Å (Cu(3)−Cu(4)).

$[Cu_2(PAHAP)(gly)_2(NO_3)(H_2O)](NO_3)\cdot 3H_2O$ (4). The structure of **4** is illustrated in Figure 5, and bond distances and angles relevant to the copper coordination spheres are given in Table 8. The metal centers are square pyramidal, with a copper−copper separation of 4.412(4) Å. The basal donor set comprises a diazine and pyridine nitrogen pair along with the amino acid

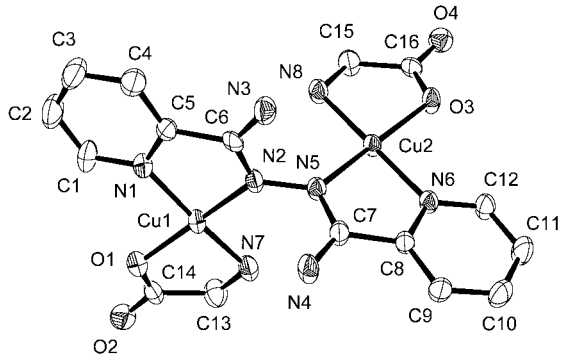

Figure 5. Structural representation for **4**, with hydrogen atoms omitted (50% probability thermal ellipsoids).

Table 8. Interatomic Distances (Å) and Angles (Deg) Relevant to the Copper Coordination Spheres in $[Cu_2(PAHAP)(gly)_2(NO_3)(H_2O)](NO_3)\cdot 3H_2O$ (**4**)

Cu(1)−O(1)	1.935(5)	Cu(2)−O(3)	1.967(4)
Cu(1)−N(7)	1.970(6)	Cu(2)−N(8)	1.977(5)
Cu(1)−N(1)	1.975(6)	Cu(2)−N(5)	1.985(5)
Cu(1)−N(2)	1.978(6)	Cu(2)−N(6)	1.987(5)
Cu(1)−O(31)	2.548(5)	Cu(2)−O(50)	2.374(8)
Cu(1)−Cu(2)	4.412(4)	N(2)−N(5)	1.409(6)

O(1)−Cu(1)−N(7)	85.2(2)	O(1)−Cu(1)−N(1)	94.4(2)
N(7)−Cu(1)−N(1)	172.9(2)	O(1)−Cu(1)−N(2)	169.1(2)
N(7)−Cu(1)−N(2)	100.9(2)	N(1)−Cu(1)−N(2)	80.7(2)
O(3)−Cu(2)−N(8)	85.10(19)	O(3)−Cu(2)−N(5)	170.1(2)
N(8)−Cu(2)−N(5)	99.6(2)	O(3)−Cu(2)−N(6)	94.66(19)
N(8)−Cu(2)−N(6)	179.6(2)	N(5)−Cu(2)−N(6)	80.7(2)
O(3)−Cu(2)−O(50)	93.4(2)	N(8)−Cu(2)−O(50)	91.2(3)
N(5)−Cu(2)−O(50)	95.2(2)	N(6)−Cu(2)−O(50)	88.4(3)

Table 9. Interatomic Distances (Å) and Angles (Deg) Relevant to the Copper Coordination Spheres in $[Cu_2((PHMAP\text{-}H)(NO_3)_3(H_2O)(MeOH)]$ (**6**)

Cu(1)−N(3)	1.955(3)	Cu(2)−N(2)	1.963(4)
Cu(1)−O(31)	1.971(11)	Cu(2)−N(5)	2.042(3)
Cu(1)−O(32)	2.00(5)	Cu(2)−O(6)	2.049(3)
Cu(1)−O(1)	2.007(3)	Cu(2)−O(9)	2.215(3)
Cu(1)−N(1)	2.016(3)	Cu(1)−Cu(2)	4.759(1)
Cu(1)−O(2)	2.153(4)	N(3)−N(4)	1.368(4)
Cu(2)−N(4)	1.944(3)		

N(3)−Cu(1)−O(31)	172.7(3)	O(1)−Cu(1)−O(2)	94.11(14)
N(3)−Cu(1)−O(32)	172.0(9)	N(1)−Cu(1)−O(2)	113.4(2)
N(3)−Cu(1)−O(1)	92.78(12)	N(4)−Cu(2)−N(2)	79.45(14)
O(31)−Cu(1)−O(1)	94.0(3)	N(4)−Cu(2)−N(5)	81.16(12)
O(32)−Cu(1)−O(1)	88.0(13)	N(2)−Cu(2)−N(5)	160.10(14)
N(3)−Cu(1)−N(1)	80.25(12)	N(4)−Cu(2)−O(6)	144.54(13)
O(31)−Cu(1)−N(1)	95.0(3)	N(2)−Cu(2)−O(6)	97.71(14)
O(32)−Cu(1)−N(1)	95.4(13)	N(5)−Cu(2)−O(6)	100.69(11)
O(1)−Cu(1)−N(1)	151.69(13)	N(4)−Cu(2)−O(9)	125.54(12)
N(3)−Cu(1)−O(2)	92.1(2)	N(2)−Cu(2)−O(9)	90.60(14)
O(31)−Cu(1)−O(2)	84.6(2)	N(5)−Cu(2)−O(9)	97.03(12)
O(32)−Cu(1)−O(2)	95.8(9)	O(6)−Cu(2)−O(9)	89.63(10)

NO pair, with in-plane distances <2.0 Å. Longer axial contacts to O(31) (Cu(1)−O(31) 2.548(4) Å), belonging to a nitrate, and a water molecule (Cu(2)−O(50) 2.374(8) Å) complete the five-coordination. The copper basal planes are twisted around the N−N bridge, with an angle of 85.2(2)° between the least-squares planes Cu(1)−N(1)−C(5)−C(6)−N(2) and Cu(2)−N(5)−C(7)−C(8)−N(6) (torsion angle Cu(1)−N(2)−N(5)−Cu(2) 90.8(4)°).

$[Cu_2(PHMAP\text{-}H)(NO_3)_3(H_2O)(MeOH)]$ (6). The structure of **6** is illustrated in Figure 6, and bond distances and angles relevant to the copper coordination spheres are given in Table 9. The ligand PHMAP acts in a pentadentate fashion, with all nitrogens acting as donors to the two five-coordinate copper(II)

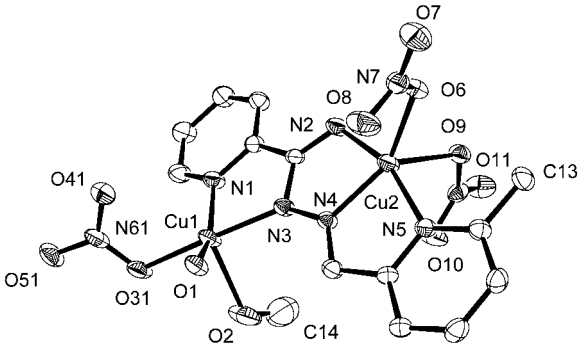

Figure 6. Structural representation for **6**, with hydrogen atoms omitted (50% probability thermal ellipsoids).

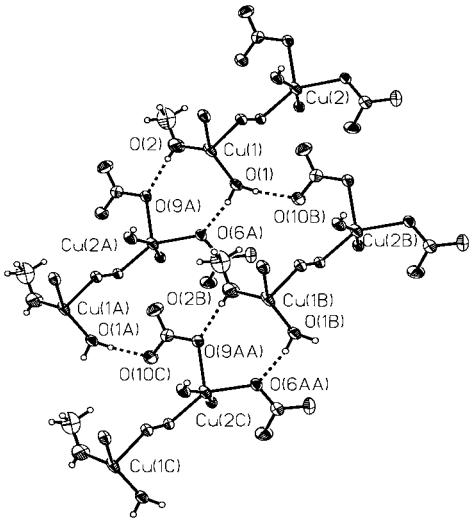

Figure 7. Two-dimensional network structure in **6**.

centers. Cu(1) binds to pyridine and diazine nitrogens N(1) and N(3), respectively, and Cu(2) is bound to pyridine, diazine, and amino nitrogens N(5), N(4), and N(2), respectively. N(2) is deprotonated. Two nitrates are bound terminally to Cu(2) and one to Cu(1), with the fourth and fifth coordination sites at Cu(1) occupied by water and methanol molecules, respectively. The nitrate bound to Cu(1) is disordered and was modeled as two nitrates with a total occupancy of 1. The stereochemistry at both Cu(1) and Cu(2) is best described as distorted square pyramidal, with τ values[41] of 0.35 and 0.26, respectively. The effect of this arrangement is to lock the ligand into an almost planar trans configuration because of the coordination of N(2), coupled with the sp^2 character at C(6), N(3), N(4), and C(7). The angle between the least-squares planes Cu(1)−N(1)−C(5)−C(6)−N(3) and Cu(2)−N(5)−C(8)−C(7)−N(4) is 168.3°. The Cu(1)−Cu(2) separation (4.759(1) Å) is large, as would be expected.

Three short intermolecular contacts link the dinuclear complexes in a two-dimensional network. This is illustrated in Figure 7 and shows the dinuclear units linked head to tail in a chain arrangement by H-bonding interactions between nitrate oxygen O(9) and methanol oxygen O(2) (O(2)−O(9) 2.749(4) Å), and between water oxygen O(1) and nitrate oxygen O(6) (O(1)−O(6) 2.732(4) Å), with the chains cross-linked by another H-bonding contact between nitrate oxygen O(10) and water oxygen O(1) (O(1)−O(10) 2.753(4) Å). Corresponding O−H−O angles fall in the range 160−177°.

$[Cu_2(PAHOX\text{-}H)_2](ClO_4)_2$ (7). The molecular structure of **7** is illustrated in Figure 8, and bond distances and angles relevant to the copper coordination spheres are listed in Table

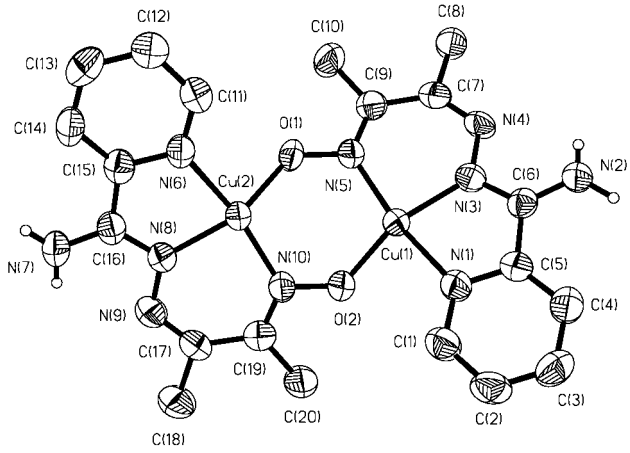

Figure 8. Structural representation for **7**, with hydrogen atoms omitted (50% probability thermal ellipsoids).

Table 10. Interatomic Distances (Å) and Angles (Deg) Relevant to the Copper Coordination Spheres in $[Cu_2((PAHOX\text{-}H)_2](ClO_4)_2$ (**7**)

Cu(1)−O(2)	1.916(2)	Cu(2)−N(6)	2.018(3)
Cu(1)−N(3)	1.934(3)	Cu(1)−Cu(2)	3.491(1)
Cu(1)−N(5)	1.937(3)	N(5)−O(1)	1.344(3)
Cu(1)−N(1)	2.024(3)	N(10)−O(2)	1.331(3)
Cu(2)−O(1)	1.891(2)	N(3)−N(4)	1.386(3)
Cu(2)−N(10)	1.930(3)	N(8)−N(9)	1.386(4)
Cu(2)−N(8)	1.934(2)		
O(2)−Cu(1)−N(3)	156.71(10)	O(1)−Cu(2)−N(10)	103.12(10)
O(2)−Cu(1)−N(5)	102.81(10)	O(1)−Cu(2)−N(8)	149.93(11)
N(3)−Cu(1)−N(5)	90.59(11)	N(10)−Cu(2)−N(8)	90.96(11)
O(2)−Cu(1)−N(1)	87.64(10)	O(1)−Cu(2)−N(6)	88.96(10)
N(3)−Cu(1)−N(1)	80.76(10)	N(10)−Cu(2)−N(6)	166.65(11)
N(5)−Cu(1)−N(1)	168.98(11)	N(8)−Cu(2)−N(6)	80.97(11)

10. The dinuclear structural arrangement in **7** involving NO bridging is the result of a compromise in the coordinating abilities of two very different portions of the same ligand. The well-documented ability of this class of N_4 dinucleating ligand to bind two metals[9,12,16,19,22] does not prevail, and the resulting mode of coordination is dominated by the oxime group. A similar coordination mode occurs in the complex $[Cu(HdoxN_2)]_2^{2+}$ (H_2doxN_2 = 4,4-diaza-3,6-dimethyl-3,5-octadiene-2,7-dione-2,7-dioxime).[42] However, with a similar N_4 ligand (pyridazine-3,6-dicarbaldehyde dioxime), involving two terminal oxime groups bound to a pyridazine, the dinucleating ability of the N_4 fragment prevails, and the oxime oxygens remain uncoordinated.[9]

The copper centers are quite distorted, with four short in-plane contacts to the nitrogen and oxygen atoms. The Cu−O contacts are very short (<1.92 Å), consistent with proton loss from the ligand OH group. Longer axial contacts between the copper centers and one perchlorate create an infinite chain structure along the *b* axis (Cu(1)−O(6) 2.458(3) Å, Cu(2)−O(4) 2.733(3) Å, Cu(1)−O(5A) 3.124(3) Å), suggesting that each copper probably should be considered as having a distorted square-pyramidal structure (Figure 9). The Cu(1)−O(5A) contact, despite being long, clearly is responsible for the chain ordering. The result of the axial perchlorate coordination is to fold the molecule and create a boat conformation in the six-membered $Cu_2N_2O_2$ ring, with an angle of 129.3° between the CuNO planes. As a result, the copper−copper separation (3.491(1) Å) is fairly short for a system of this sort. An additional contact involving a hydrogen bond between amino

(42) Abraham, F.; Capon, J. M.; Nowogrocki, G.; Sueur, S.; Brémard, C. *Polyhedron* **1985**, *4*, 1761.

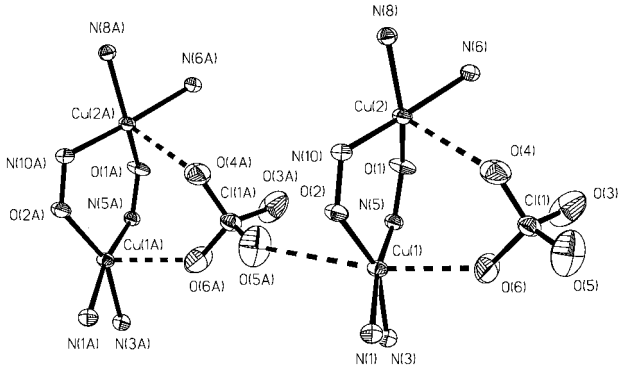

Figure 9. Chain structure in **7** associated with axial perchlorate bridging interaction.

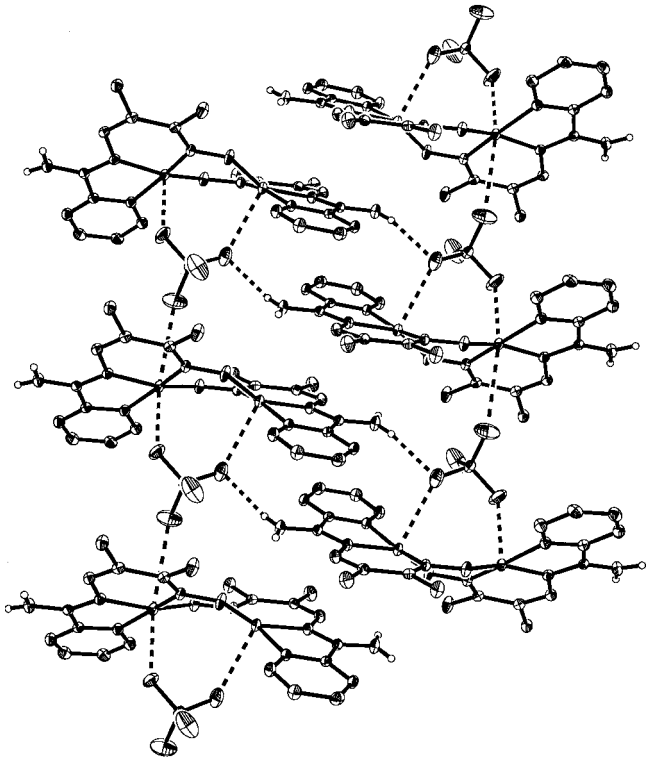

Figure 10. Double-stranded chain structure in **7**.

hydrogen H(71N) and perchlorate oxygen O(4B) (H(71N)−O(4B) 2.20(4) Å, N(7)−O(4B) 2.958(4) Å, N(7)−H(71N)−O(4B) 158(4)°) links the chains in pairs with a double-stranded arrangement (Figure 10).

[Cu(PAHOX)(SO$_4$)]$_2$·2H$_2$O (8). The molecular structure of **8** is illustrated in Figure 11, and bond distances and angles relevant to the copper coordination sphere are listed in Table 11. The bonding mode of the ligand PAHOX is similar to that in **7**, creating adjacent five- and six-membered chelate rings, but the oxygen of the N−OH group is not bonded to an adjacent copper. This equivalent basal position in **8** is occupied by an oxygen of a μ_2-SO$_4$, which bridges the two square-pyramidal copper centers, with another oxygen occupying the axial site in the adjacent copper. The basal copper−nitrogen and copper−oxygen distances are short (<2.01 Å), with a somewhat longer axial contact to a sulfate oxygen (Cu(1)−O(5) 2.199(3) Å). The ligand bonding arrangement resembles that in [Cu(PMK)(NO$_3$)$_2$],[19] which is a mononuclear complex with an axial and equatorial monodentate nitrate. The copper atom in **8** is displaced form the mean basal ligand plane toward the sulfate oxygen by 0.338 Å. The two sulfate bridges form an unusual

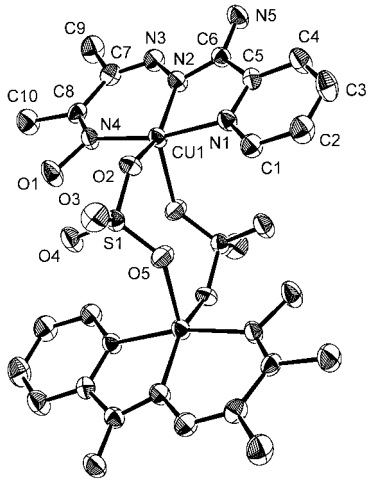

Figure 11. Structural representation for **8**, with hydrogen atoms omitted (50% probability thermal ellipsoids).

Table 11. Interatomic Distances (Å) and Angles (Deg) Relevant to the Copper Coordination Spheres in [Cu(PAHOX)(SO$_4$)]$_2$·2H$_2$O (**8**)

Cu(1)−O(2)	1.972(3)	S(1)−O(5)	1.464(3)
Cu(1)−O(5)	2.199(3)	N(2)−N(3)	1.376(4)
Cu(1)−N(1)	1.995(3)	N(2)−C(6)	1.319(5)
Cu(1)−N(2)	1.934(3)	N(3)−C(7)	1.284(5)
Cu(1)−N(4)	2.009(3)	Cu(1)−Cu(1)a	4.992(1)
S(1)−O(2)	1.491(3)		
O(2)−Cu(1)−O(5)	100.0(1)	N(1)−Cu(1)−N(2)	81.5(1)
O(2)−Cu(1)−N(1)	89.9(1)	N(1)−Cu(1)−N(4)	167.8(1)
O(2)−Cu(1)−N(2)	150.9(1)	N(2)−Cu(1)−N(4)	88.0(1)
O(2)−Cu(1)−N(4)	96.4(1)	O(2)−S(1)−O(5)	109.6(2)
O(5)−Cu(1)−N(1)	101.9(1)	Cu(1)−O(2)−S(1)	135.1(2)
O(5)−Cu(1)−N(2)	109.0(1)	Cu(1)−O(5)−S(1)	135.9(2)
O(5)−Cu(1)−N(4)	87.3(1)		

chairlike eight-membered chelate ring, bridging the two copper atoms with a Cu−Cu distance of 4.992(1) Å. This is a most unusual sulfate bridging arrangement, and while μ_2-SO$_4$ groups can bridge two metal centers in a chelating intramolecular fashion,[43−45] and in a bidentate chain bridging arrangement,[46] the current intermolecular bridging mode is rare. One similar example occurs in the structure [Cu(oaoH$_2$)(H$_2$O)(SO$_4$)]$_2$, (oaoH$_2$ = oxamide oxime), in which the copper−copper separation is 5.087(2) Å and the two sulfate bridges link the square-pyramidal coppers in a similar axial/equatorial fashion.[47]

Spectroscopy and Magnetism. Compound **1** exhibits two ν_{NH} infrared bands at 3328 and 3176 cm^{-1} associated with the NH$_2$ groups in PAHAP, and three prominent ν_{CN} bands at 2100, 2083, and 2059 cm^{-1} consistent with the cis arrangement of two isothiocyanates at each copper center. A broad, strong absorption at 1639 cm^{-1} is associated with both coordinated and lattice DMF. In the visible absorption region, a broad single band is observed at 675 (solid) and 680 nm (DMF solution). **2** exhibits two ν_{NH} bands at 3329 and 3175 cm^{-1} associated with the NH$_2$ groups in PAHAP, a broad band at 3500 cm^{-1} due to lattice water, and a prominent ($\nu_1 + \nu_4$)[48] nitrate band at 1748 cm^{-1}. At least two nitrate combination bands would be expected, associated with the lattice and coordinated nitrates,

(43) Knuuttila, P. *Inorg. Chim. Acta* **1982**, *58*, 201.
(44) Thompson, L. K.; Hanson, A. W.; Ramaswamy, B. S. *Inorg. Chem.* **1984**, *23*, 2459.
(45) Barraclough, C. G.; Tobe, M. L. *J. Chem. Soc.* **1961**, 1993.
(46) Korvenranta, J. *Suom. Kemistil. B* **1973**, *46*, 240.
(47) Endres, H.; Nöthe, D.; Rossato, E.; Hatfield, W. E. *Inorg. Chem.* **1984**, *23*, 3467.
(48) Lever, A. B. P.; Mantovani, E.; Ramaswamy, B. S. *Can. J. Chem.* **1971**, *49*, 1957.

but very strong $\nu_{C=N}$ bands at 1672 and 1648 cm^{-1} dominate this region. A broad visible band in the solid state at 725 nm remains essentially unchanged in DMF but shifts to 740 nm in H_2O, suggesting solvent coordination.

The infrared spectrum of **3** above 3100 cm^{-1} is dominated by bands associated with water (3512 cm^{-1}) and NH_2 groups (3360 cm^{-1}). Nitrate combination bands are masked by a strong carboxylate absorption at 1685 cm^{-1} associated with the alaninate groups. A strong, broad visible absorption at 610 nm in the solid state is shifted to slightly lower energy (640 nm) in aqueous solution, consistent with square-pyramidal geometry and little change in solution. **4** exhibits a broad absorption at 3500 cm^{-1} due to coordinated and lattice water and a band at 3363 cm^{-1} associated with the NH_2 groups. Bands at 1684 and 1603 cm^{-1} are associated with unidentate carboxylate, and bands at 1664 and 1639 cm^{-1} are due to CN stretch. Visible absorptions are found at 630 nm in the solid state, and at 640 and 600 nm respectively in water and DMF solution, again consistent with square-pyramidal geometry and little change in solution.

5 shows only infrared absorptions at high energy associated with the NH_2 groups (3364, 3266 cm^{-1}), and a very strong ν_{CN} band at 2215 cm^{-1} associated with terminal N-bonded cyanate. A strong band at 1676 cm^{-1} is consistent with lattice DMF. A broad visible absorption in the solid-state electronic spectrum at 650 nm shifts slightly (630 nm) in DMF solution, consistent with a distorted square-planar stereochemistry at copper. This band is at substantially higher energy than in **1**, which has square-pyramidal copper(II) centers.

A single ν_{NH} band at 3347 cm^{-1} in the infrared spectrum of **6** confirms the deprotonation at N(2) and the anionic nature of the ligand, and a broad shoulder at 3600 cm^{-1} is associated with the coordinated water molecule. A complex group of (ν_1 + ν_4) nitrate bands[48] is observed (1777, 1744, 1735(sh), 1721(sh), and 1712 cm^{-1}), consistent with the three slightly different monodentate nitrate groups. A broad visible band in the solid sate at 695 nm is shifted to slightly lower energies in water (710 nm) and DMF (715 nm), consistent with metal ion solvation.

Several ν_{NH} bands are observed in the infrared spectrum of **7** (3387, 3297, 3235 cm^{-1}), confirming the existence of a free NH_2 group, and there is no higher energy band due to ν_{OH}. In the ν_3 Cl−O stretching region, three dominant perchlorate bands are observed at 1109, 1050, and 1011 cm^{-1}, but expansion of this region reveals further fine structure and a total of seven bands. The three main bands are sensibly assigned to the bridging perchlorate connecting the two copper centers in an intramolecular fashion, associated with nominal C_{2v} local site symmetry. The additional bands are possibly due to the asymmetric nature of this bridge and the additional bridging interactions (Figure 10). Visible absorptions for **7** are difficult to resolve, with a broad shoulder occurring at about 600 nm in both solid and solution.

The high-energy region of the infrared spectrum of **8** is dominated by a strong, sharp band at 3620 cm^{-1} (ν_{OH}; N−OH) and ν_{NH} bands at 3440 and 3247 cm^{-1} due to the free NH_2 group. A very complex absorption envelope is observed in the range 989−1172 cm^{-1}, with a total of 11 resolvable bands. These are clearly associated with the ν_3 sulfate vibration, split as a result of reduced symmetry in the unusual bridging mode. **8** exhibits a broad visible band in the solid state at 660 nm, which shifts to higher energy (595 nm) in water but to lower energy (715 nm) in DMF, indicative of a significant structural change in solution.

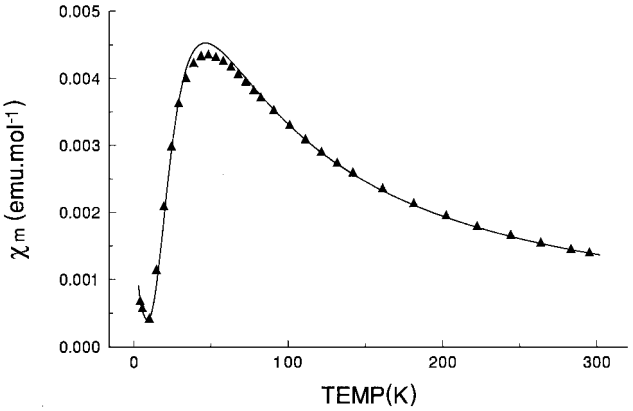

Figure 12. Variable-temperature magnetic data for **1**. The solid line represents the best fit of the experimental data to eq 1, with g = 2.107(1), $-2J$ = 51.1(3) cm^{-1}, ρ = 0.006, $N\alpha = 75 \times 10^{-6}$ emu, θ = −1.4 K, 10^2R = 1.7 ($R = [\Sigma(\chi_{obs} - \chi_{calc})^2/\Sigma\chi_{obs}^2]^{1/2}$).

Variable-temperature magnetic susceptibility data were collected for powdered samples of all the complexes and taken from the same uniform batches used for structural determination (**1**−**4**, **6**−**8**). The samples were predried under vacuum in order to prevent possible mass loss during sample preparation prior to a variable temperature run. In those cases where obvious desolvation occurred elemental analyses were repeated. Compound **1** has a room-temperature magnetic moment (ν_{eff} = 1.78 μ_B) close to the spin-only value for Cu^{2+} but displays a maximum in the χ_m versus temperature profile (Figure 12) indicative of weak antiferromagnetic coupling. The data were fitted to the Bleaney−Bowers equation (eq 1)[49] ($H = -2J\hat{S}_1.\hat{S}_2$).

$$\chi_m = \frac{N\beta^2g^2}{3k(T-\theta)}[1 + {}^1/_3\exp(-2J/kT)]^{-1}(1-\rho) + \frac{(N\beta^2g^2)\rho}{4kT} + N\alpha \quad (1)$$

$2J$ is the singlet−triplet splitting, and other terms have their usual meaning (χ_m is expressed per mole of copper atoms, $N\alpha$ is the temperature-independent paramagnetism, θ is a Weiss-like corrective term for weak intermolecular associations,[50,51] and ρ represents the fraction of a magnetically dilute impurity). The parameters giving the best fit were obtained using a nonlinear regression analysis with g, J, ρ, θ, and $N\alpha$ as variables. The solid line in Figure 12 represents the best-fit situation with g = 2.107(1), $-2J$ = 51.1(3) cm^{-1}, ρ = 0.006, $N\alpha = 75 \times 10^{-6}$ emu, θ = −1.4 K, 10^2R = 1.7 ($R = [\Sigma(\chi_{obs} - \chi_{calc})^2/\Sigma\chi_{obs}^2]^{1/2}$). Compound **2** has a higher room-temperature magnetic moment (μ_{eff} = 1.91 μ_B), and the χ_mT values are larger than 0.41 emu·mol^{-1}·K throughout the 5−300 K temperature range, indicative of no net coupling between the copper centers. Compound **3** has a room-temperature magnetic moment (μ_{eff} = 1.77 μ_B) close to the spin-only value, but a plot of χ_m versus temperature shows a maximum at ≈40 K (Figure 13), indicative of intramolecular antiferromagnetic coupling. Fitting of the variable-temperature data to eq 1 gives g = 2.076(3), $-2J$ = 45.6(4) cm^{-1}, ρ = 0.0382, $N\alpha = 75 \times 10^{-6}$ emu, θ = −3.6 K, 10^2R = 0.93. The solid line in Figure 13 was calculated using

(49) Bleaney, B.; Bowers, K. D. *Proc. R. Soc. London, Ser. A* **1952**, *214*, 451.
(50) McGregor, K. T.; Barnes, J. A.; Hatfied, W. E. *J. Am. Chem. Soc.* **1973**, *95*, 7993.
(51) Sikorav, S.; Bkouche-Waksman, I.; Kahn, O. *Inorg. Chem.* **1984**, *23*, 490.

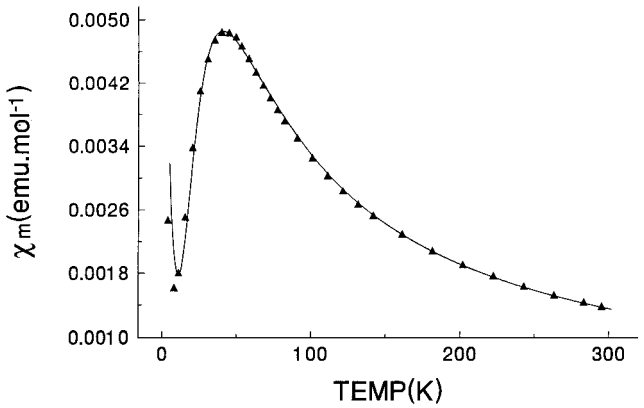

Figure 13. Variable-temperature magnetic data for **3**. The solid line represents the best fit of the experimental data to eq 1, with $g = 2.076(3)$, $-2J = 45.6(4)$ cm^{-1}, $\rho = 0.0382$, $N\alpha = 75 \times 10^{-6}$ emu, $\theta = -3.6$ K, $10^2R = 0.93$ ($R = [\Sigma(\chi_{obs} - \chi_{calc})^2/\Sigma\chi_{obs}^2]^{1/2}$).

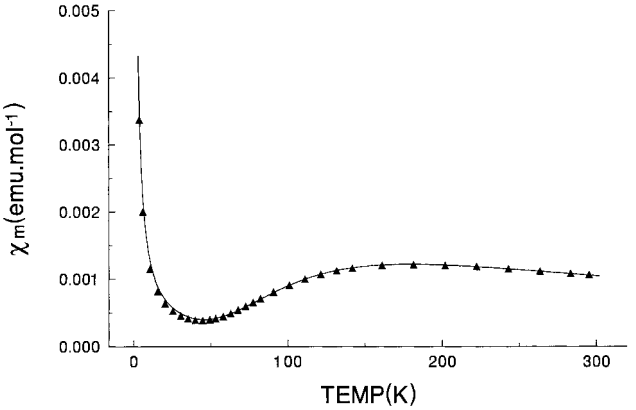

Figure 14. Variable-temperature magnetic data for **6**. The solid line represents the best fit of the experimental data to eq 1, with $g = 2.097(12)$, $-2J = 208(2)$ cm^{-1}, $\rho = 0.031$, $N\alpha = 66 \times 10^{-6}$ emu, $\theta = 0$ K, $10^2R = 0.64$ ($R = [\Sigma(\chi_{obs} - \chi_{calc})^2/\Sigma\chi_{obs}^2]^{1/2}$).

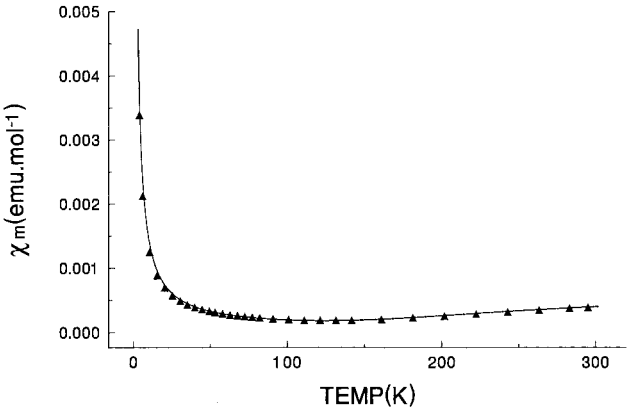

Figure 15. Variable-temperature magnetic data for **7**. The solid line represents the best fit of the experimental data to eq 1, with $g = 2.069(22)$, $-2J = 549(6)$ cm^{-1}, $\rho = 0.035$, $N\alpha = 49 \times 10^{-6}$ emu, $\theta = -1.0$ K, $10^2R = 1.7$ ($R = [\Sigma(\chi_{obs} - \chi_{calc})^2/\Sigma\chi_{obs}^2]^{1/2}$).

these parameters. A somewhat larger than usual Weiss-like correction was required to give a reasonable data fit, implying a possible intermolecular antiferromagnetic exchange component. One reasonably short contact (2.742 Å) between the two molecules in the structure occurs between O(5) (axial water bound to Cu(1)) and O(10), which is the nonbonded carbonyl oxygen in the alaninate residue bound equatorially to Cu(4).

Compound **4** has a room-temperature (295 K) magnetic moment of 1.86 μ_B, suggesting very weak coupling or no exchange at all. A plot of $\chi_m T$ versus temperature shows a gradual drop from a room-temperature value of 0.44 emu·mol^{-1}·K to a value of 0.30 emu·mol^{-1}·K at 4.5 K. This indicates the possible presence of very weak antiferromagnetic exchange. The data were fitted to eq 1 to give $g = 2.09(1)$, $-2J = 1.5(3)$ cm^{-1}, $\rho = 0.0007$, $N\alpha = 72 \times 10^{-6}$ emu, $\theta = -0.8$ K, $10^2R = 3.5$. This is not a good fit, and, since the singlet−triplet splitting is very small and comparable with the Zeeman energy ($g\beta$H), the data were also fitted to the magnetization expression (eqs 2 and 3), corrected for interdimer

$$M = Ng\beta(\sinh(g\beta H/kT))/(\exp(-2J/kT) + 2\cosh(g\beta H/kT) + 1) \quad (2)$$

$$\chi_m = M/H + N\alpha \quad (3)$$

exchange (zJ').[52,53] Comparable fitting parameters were obtained by this method, with a slightly improved fit ($g = 2.103(7)$, $-2J = 1.4(5)$ cm^{-1}, $zJ' = -1.44$ cm^{-1}, $N\alpha = 60 \times 10^{-6}$ emu, $\rho = 0.0005$), confirming the very weak antiferromagnetic exchange.

Compound **5** has a room-temperature moment of 1.76 μ_B, close to the spin-only value for copper(II). However, the χ_m versus temperature profile has a maximum at 100 K, indicating significant antiferromagnetic coupling between the copper(II) centers, which are clearly bridged by the N−N diazine group. The data were fitted to eq 1 to give $g = 2.25(5)$, $-2J = 128(4)$ cm^{-1}, $\rho = 0.012$, $N\alpha = 66 \times 10^{-6}$ emu, $\theta = -2.4$ K, $10^2R = 0.64$. Compared with **1**, the exchange is much larger, suggesting a large dihedral angle between the copper coordination planes (>103.6°). This may well be associated, in part, with the apparent absence of coordinated DMF in this compound, leading to different steric repulsion effects. The significant negative θ value implies a weak intermolecular antiferromagnetic interaction, but this cannot be evaluated without structural information.

Compound **6** has a room-temperature magnetic moment ($\mu_{eff} = 1.53$ μ_B) well below the spin-only value and indicative of significant antiferromagnetic coupling. The variable-temperature susceptibility profile (Figure 14) displays a maximum at about 180 K, and fitting to eq 1 gives $g = 2.097(12)$, $-2J = 208(2)$ cm^{-1}, $\rho = 0.031$, $N\alpha = 66 \times 10^{-6}$ emu, $\theta = 0$ K, $10^2R = 0.64$. The solid line in Figure 14 was calculated with these parameters. The sharp rise in susceptibility at low temperature is indicative of a significant proportion of paramagnetic impurity (3.1%). The extensive hydrogen-bonding network in this compound (Figure 7) does not appear to provide any intermolecular contribution to the exchange situation. Compound **7** has a very low room-temperature magnetic moment ($\mu_{eff} = 0.88$ μ_B), indicating strong antiferromagnetic coupling between the copper(II) centers. The susceptibility versus temperature profile (Figure 15) shows a rise in χ_m approaching 300 K, but no maximum, and a sharp rise in χ_m at low temperature, indicating significant paramagnetic impurity. Analysis of the data using eq 1 gives $g = 2.069(22)$, $-2J = 549(6)$ cm^{-1}, $\rho = 0.035$, $N\alpha = 49 \times 10^{-6}$ emu, $\theta = -1.0$ K, $10^2R = 1.7$ for the best-fit line (Figure 15). The negative θ value suggests the presence of a weak intermolecular antiferromagnetic component. This could be associated with the perchlorate and hydrogen-bonding bridging interactions, but these are nominally orthogonal in nature. Compound **8** has a room-temperature magnetic moment

(52) Myers, B. E.; Berger, L.; Friedberg, S. J. *J. Appl. Phys.* **1969**, *40*, 1149.
(53) Marsh, W. E.; Patel, K. C.; Hatfield, W. E.; Hodgson, D. J. *Inorg. Chem.* **1983**, *22*, 511.

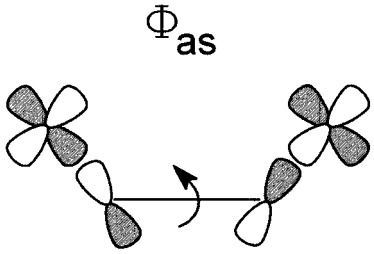

Figure 16. Representation of the antisymmetric molecular orbital combination involving the metal $d_{x^2-y^2}$ orbitals and the nitrogen *p* orbitals.

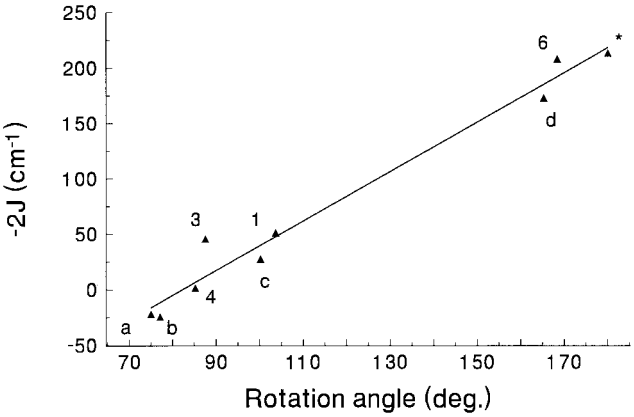

Figure 17. Plot of $-2J$ (cm^{-1}) against magnetic plane rotational angle for **1**, **3**, **4**, and **6**: $[Cu_2(PAHAP)X_4]\cdot H_2O$ (X = Cl, Br; a, b), $[Cu_2(PAHAP)(H_2O)_6](NO_3)_4$ (c), $[Cu_2(PMHAP\text{-}H)(NO_3)_3]$ (d)[18] (*, from ref 23). The solid line corresponds to eq 4.

(μ_{eff}) of 1.85 μ_B, suggesting no coupling, and this is confirmed by the $\chi_m T$ versus temperature profile, which shows a constant $\chi_m T$ value of 0.42 throughout the 4−300 K temperature range.

In a previous magnetostructural study,[18] the magnetic properties of this type of dicopper(II) complex, in which the two copper(II) centers are linked by a N−N single bond fragment, were related directly to the angle of rotation of the copper magnetic planes about the N−N bond and the alignment of the nitrogen *p* orbitals. Spin exchange was associated with a σ interaction between the copper magnetic orbitals via the N−N bond (Figure 16 depicts a representation of the antisymmetric molecular orbital combination involving the metal $d_{x^2-y^2}$ orbitals and the nitrogen p orbitals). The results were supported by extended Hückel calculations[54] on real molecules and also appropriately chosen models. For copper centers with $d_{x^2-y^2}$ ground states, rotation angles $<\approx 80°$ led to ferromagnetic behavior, while for large angles antiferromagnetic behavior was observed. The magnetostructural data for the compounds described in the previous study and compounds **1**, **3**, **4**, and **6** from the present study, in addition to one literature compound appropriate to the series[23] (all have $d_{x^2-y^2}$ magnetic ground states), are plotted in Figure 17. There is a fairly good straight line relationship between exchange integral and magnetic plane rotation angle over a 105° angle range. Linear regression of the data gives eq 4 (α = rotation angle).

$$-2J = 2.233\alpha - 183.7\ \text{cm}^{-1} \qquad (4)$$

Equation 5 shows the relationship between total exchange *J*, the inherent ferromagnetic component J_F, and the antiferromagnetic term J_{AF}, based on the orbital model for the exchange interaction.[55−57] The denominator in the J_{AF} term, which

$$J = J_F + J_{AF} = -2K_{12} + (\epsilon_s - \epsilon_a)^2/(J_{11} - J_{12}) \qquad (5)$$

involves Coulomb integrals of the localized molecular orbitals, is considered to be invariant within a related series of compounds, and so $(\epsilon_s - \epsilon_a)^2$ effectively controls the antiferromagnetic term. At the point where $\epsilon_s = \epsilon_a$, J_{AF} is zero (the point of effective orthogonality of the magnetic orbitals), and so ferromagnetic behavior would be expected. In fact, for small ($\epsilon_s - \epsilon_a$) values greater than zero, *J* can still be positive (i.e., ferromagnetic behavior prevails), depending on the magnitude of J_F.

It is clear that the most important feature responsible for antiferromagnetic coupling is the degree of overlap of the copper magnetic orbitals via the p orbitals on the nitrogen atoms of the N−N bridge. Any inherent ferromagnetic exchange would reasonably be expected to be roughly constant throughout this series, since all that occurs, in essence, is a rotation about the N−N bond, with a separation of the metal centers which falls in a fairly narrow range (3.8−4.8 Å). The observed changes in magnetic properties can, therefore, be associated with a variation in the antiferromagnetic exchange component only. The theoretical extended Hückel study[18] on closely related model compounds indicates that effective orthogonality of the copper magnetic orbitals occurs at about a 70° rotational angle ($\epsilon_s = \epsilon_a$). Using eq 4, the corresponding exchange term for such an angle is 27 cm^{-1}. This suggests, therefore, that, for the compounds $[Cu_2(PAHAP)X_4]\cdot H_2O$ (X = Cl, Br),[18] the measured exchange ($2J$ = 24.4(2), 22(2) cm^{-1}, respectively) is a reflection of "real" ferromagnetic behavior for two copper(II) centers separated by ≈3.8 Å and essentially unencumbered by the presence of antiferromagnetism.

Compounds **1**−**4**, **6** have related structures, with N_2 bridges linking two copper(II) centers, and widely varying rotation angles of the CuN_2C_2 chelate rings (103.6° (**1**), 119.8° (**2**), 87.5°-(average) (**3**), 85.2° (**4**), and 168.3° (**6**)). **1**, **3**, **4**, and **6** have $d_{x^2-y^2}$ ground states, and all exhibit antiferromagnetic behavior, consistent with the previous examples. It is apparent from Figure 17 that **3** diverges slightly from the straight line, with a somewhat larger than expected antiferromagnetic coupling. Compound **2** is clearly anomalous, with a large rotation angle (119.8°), but is uncoupled. Examination of the copper ion stereochemistry reveals why. The geometry at the copper centers is quite distorted but is closer to a trigonal-bipyramid (vide infra) than a square-pyramid, with the two coppers bridged through the N−N linkage via the equatorial lobes of their d_{z^2} orbitals. This component of the d_{z^2} orbital carries a small proportion of the unpaired electron density, which is consistent with the observed magnetic properties. ($\epsilon_s - \epsilon_a$) values were calculated for **1**−**4**, **6** using extended Hückel methods[54] and exact crystallographic coordinates (**1**, 155 meV; **2**, 47 meV; **3**, 104 meV; **4**, 98 meV; **6**, 377 MeV). The smallest value for **2** is entirely consistent with the magnetic properties and the related structure. The higher values associated with the other compounds are consistent with their magnetic properties and the associated rotation angles.

Compound **7** is very strongly coupled ($-2J$ = 549(6) cm^{-1}) but belongs to a different class of symmetrically bis-μ_2-NO-bridged systems. Reports of magnetic studies on such dicop-

(54) Mealli, C.; Proserpio, D. M. *J. Chem. Educ.* **1990**, *67*, 399.
(55) Hay, P. J.; Thibeault, J. C.; Hoffmann, R. *J. Am. Chem. Soc.* **1975**, *97*, 4884.
(56) Kahn, O.; Briat, B. *J. Chem. Soc., Faraday Trans.* **1976**, *72*, 268.
(57) Kahn, O.; Briat, B. *J. Chem. Soc., Faraday Trans.* **1976**, *72*, 1441.

per(II) systems are limited, but strong antiferromagnetic coupling is typical. The symmetrically N−O-bridged complex ion $[Cu(DAPDH)]_2^{2+}$ [Cu(NO)(ON)Cu] has a room-temperature magnetic moment of 0.6 μ_B,[58] indicative of strong antiferromagnetic coupling, while the asymmetrically bridged iodo complex $[LCu(PyA)_2Cu(I)]ClO_4 \cdot CH_3CN$ [Cu(NO)(NO)Cu] (L = 1,4,7-trimethyl-1,4,7-triazacyclononane; PyA = monanion of pyridine-2-aldoxime)[59] exhibits very strong antiferromagnetic coupling ($-2J > 1000$ cm^{-1}). The copper−copper separation in this complex (3.45 Å) is comparable with that in **7**, and it exhibits a similar boat-shaped structure, with an angle of 120° between the copper mean planes. It is not immediately obvious why the exchange situation for these two complexes is so different, but from a structural perspective it appears that the asymmetric $(NO)_2$ bridging arrangement provides the stronger coupling. Extended Hückel[54] calculations on **7** show two triplet-state molecular orbitals with a high degree of alignment of the copper d orbitals and the nitrogen and oxygen p orbitals in the dicopper chelate ring. A ΔE value of 82 meV is large enough to corroborate the antiferromagnetic exchange situation, but no comparison can be made with **1**, **3**, **4**, and **6**.

Compound **8** is completely uncoupled, consistent with the axial/equatorial arrangement of bonds to the sulfate bridges, leading to effective orthogonality between the copper magnetic orbitals. This is in good agreement with the magnetic study on $[Cu(oaoH_2)(H_2O)(SO_4)]_2$, which is very weakly antiferromagnetically coupled ($-2J = 2.55$ cm^{-1}).[47]

Conclusion

Additional examples of dicopper(II) complexes with single N−N bridges are reported. Their magnetic properties are consistent with a previously published model which relates magnetic exchange to the rotation of the copper magnetic planes about the N−N bond and the alignment of the diazine nitrogen p orbitals. A linear relationship is found between the rotation angle and the exchange integral over a 105° range. This alignment is controlled mostly by the coligands bound to the copper centers, which exert primarily steric effects resulting in rotation of the copper magnetic planes about the N−N bond. This creates an unusual opportunity to exert control over the magnetic properties of an exchange-coupled system and, in this case, to specifically produce systems exhibiting ferromagnetism.

Acknowledgment. We thank the Natural Sciences and Engineering Research Council of Canada for financial support for this study. The preliminary structures of **1** and **2** were carried out by Dr. G. A. P. Yap at the University of Windsor using a Siemens 3-circle diffractometer with a CCD area detector.

Supporting Information Available: Tables listing detailed crystallographic data, atomic positional parameters, anisotropic thermal parameters, and bond lengths and angles (39 pages). Ordering information is given on any current masthead page.

IC9715198

(58) Nicholson, G. A.; Lazarus, C. R.; McCormick, B. J. *Inorg. Chem.* **1980**, *19*, 192.
(59) Chaudhuri, P.; Winter, M.; Flörke, U.; Haupt, H.-J. *Inorg. Chim. Acta* **1995**, *232*, 125.